DETERMINATION OF BURST PRESSURE OF DEFECTIVE STEEL PIPES USING FINITE ELEMENT ANALYSIS

MOHAMAD ZULFADLI BIN MOHAMAD RANI

BACHELOR OF MECHANICAL ENGINEERING

UNIVERSITI MALAYSIA PAHANG

DETERMINATION OF BURST PRESSURE OF DEFECTIVE STEEL PIPES USING FINITE ELEMENT ANALYSIS

MOHAMAD ZULFADLI BIN MOHAMAD RANI

Thesis submitted in fulfilment of the requirements
for the award of the degree of
Bachelor of Mechanical Engineering

Faculty of Mechanical Engineering
UNIVERSITI MALAYSIA PAHANG

JUNE 2012

UNIVERSITI MALAYSIA PAHANG
FACULTY OF MECHANICAL ENGINEERING

I certify that the project entitled "*Determination of Burst Pressure of Defective Steel Pipes using Finite Element Analysis*" is written by *Mohamad Zulfadli Bin Mohamad Rani*. I have examined the final copy of this project and in our opinion; it is fully adequate in terms of scope and quality for the award of the degree of Bachelor of Engineering. I herewith recommend that it be accepted in partial fulfilment of the requirements for the degree of Bachelor of Mechanical Engineering.

(Juliawati Binti Alias)
Examiner Signature

SUPERVISOR'S DECLARATION

I hereby declare that I have checked this project and in my opinion, this project is adequate in terms of scope and quality for the award of the degree of Bachelor of Mechanical Engineering.

Signature: .....

Name of Supervisor: NASRUL AZUAN BIN ALANG

Position: LECTURER

Date: 25 JUNE 2012

STUDENT'S DECLARATION

I hereby declare that the work in this project is my own except for quotations and summaries which have been duly acknowledged. The project has not been accepted for any degree and is not concurrently submitted for award of other degree.

Signature: .....

Name: MOHAMAD ZULFADLI BIN MOHAMAD RANI

ID Number: MA 08090

Date: 25 JUNE 2012

IN THE NAME OF ALLAH, THE MOST BENEFICENT, THE MOST MERCIFUL

I dedicate this to my parents, supervisor, friends and
Corrosion and Fracture Focus Group of UMP for continuous moral support to complete this thesis and my bachelor degree study.

ACKNOWLEDGEMENTS

I am grateful and would like to express my sincere gratitude to my supervisor Mr. Nasrul Azuan Bin Alang for his outstanding ideas, guidance, persistent encouragement and constant support in making this thesis possible. He has always impressed me with his outstanding professional conduct, his strong conviction for science, and his belief that a Bachelor Degree program is only a start of a life-long learning experience. I am truly grateful for his progressive vision about my training in science, his tolerance of my mistakes, and his commitment to my future career. I acknowledge my sincere gratitude to my parents for their love, dream and sacrifice throughout my time as their son. I cannot find the appropriate words that could properly describe my appreciation for their devotion, support and faith in my ability to attain my goals. I would like to acknowledge their comments and suggestions, which was crucial for the successful completion of this study. My sincere thanks go to all my lab mates and members of the staff of FACULTY OF MECHANICAL ENGINEERING, UMP, who helped me in many ways. Special thanks to the member of CORROSION AND FRACTURE FOCUS GROUP for their excellent co-operation, inspirations and supports during this study.

ABSTRACT

This thesis deals with assessment of defective API 5L X65 steel pipes which are widely used in product transportation in oil and gas industry. The objective of the thesis is to determine the burst pressure of defective API X65 steel pipes under the effect of gouge length for different pipe diameter. The thesis describes the finite element analysis techniques to predict the true fracture and identify the critical locations of the structures (pipe). One-quarter three-dimensional solid modelling of steel pipe was developed using the MSC Patran 2008r1 that act as a pre-processor. The finite element analysis was then performed using MSC Marc. The finite element model of the pipe was analyzed using the non-linear isotropic elasto-plastic material that obeys the incremental of plastic theory. The values of principal stresses and strains acted on the critical location of gouge defect had been obtained by MSC Patran as a post-processor. The values were used to determine the true fracture strain which is known to be exponentially dependent to the stress triaxiality. Finally, burst pressure was determined as the true fracture strain exceeds the value of equivalent strain at that instant point. Based on the results, it is observed that the analysis using SMCS model yields more conservative burst pressure prediction. The obtained results indicate that the shorter gouge length would gives higher burst pressure which means, higher pressure needed as the pipe to experience failure at the gouge defect area. Result shows that the burst pressure decreases with increment of pipe diameter. The results concluded that the shorter gouge length and smaller pipe diameter conditions give the highest pressure value of pipe burst. Therefore, the defect characteristic is the promising criteria to increase the fitness of service of the pipe.

ABSTRAK

Tesis ini berkaitan dengan penilaian kecacatan bagi paip keluli API 5L X65 yang digunakan secara meluas untuk pengangkutan produk dalam industri minyak dan gas. Objektif tesis ini adalah untuk menentukan tekanan maksimum yang boleh ditanggung oleh paip keluli API X65 yang mengandungi kecacatan (gouge) dengan diameter paip yang berbeza. Tesis menerangkan teknik-teknik analisis unsur terhingga untuk meramalkan patah sebenar dan mengenal pasti lokasi kritikal struktur (paip). Satu-perempat tiga-dimensi pemodelan paip keluli telah dibangunkan dengan menggunakan MSC Patran 2008r1 yang bertindak sebagai pra-pemproses. Analisis unsur terhingga telah dilakukan menggunakan penyelesai MSC Marc. Model unsur terhingga paip telah dianalisis dengan menggunakan bahan yang mempunyai ciri-ciri isotropi elastic-plastik yang mengikut kepada peningkatan teori plastik. Nilai-nilai tegasan dan terikan utama bertindak di lokasi kritikal kecacatan telah diperolehi oleh MSC Patran yang digunakan sebagai pasca-pemproses. Nilai-nilai tersebut telah digunakan untuk menentukan terikan patah sebenar yang juga eksponen bergantung kepada tekanan tiga paksi. Akhirnya, tekanan pecah ditentukan sebagai terikan patah benar melebihi nilai terikan pada titik tersebut. Berdasarkan keputusan, ia diperhatikan bahawa analisis yang menggunakan model SMCS menghasilkan ramalan tekanan pecah yang lebih konservatif. Keputusan yang diperolehi menunjukkan bahawa kecacatan (gouge) yang lebih pendek akan memberikan tekanan pecah yang lebih tinggi. Keputusan menunjukkan bahawa tekanan pecah berkurangan dengan pembesaran saiz paip. Keputusan yang diperolehi menyimpulkan bahawa kecacatan yang pendek dan diameter paip yang lebih kecil memberikan nilai tekanan tertinggi sebelum paip pecah. Oleh itu, ciri-ciri kecacatan adalah kriteria yang menjanjikan untuk keselamatan paip yang boleh digunakan.

TABLE OF CONTENTS

CHAPTER 4 RESULTS AND DISCUSSION

CHAPTER 5 CONCLUSION AND RECOMMENDATIONS

LIST OF TABLES

LIST OF FIGURES

LIST OF FORMULA

LIST OF SYMBOLS

σ	Stress
σ_u	Ultimate Tensile Strength
σ_y	Yield Strength
σ_h	Hoop Stress
σ_r	Radial Stress
σ_l	Longitudinal Stress
ε	Strain
ε_{ef}	True Fracture Strain
E	Young Modulus
v	Poisson Ratio
λ	Shell Parameter
M_t	Folias Stress Magnification Factor
π	PI
τ	Shear Stress

LIST OF ABBREVIATIONS

API	American Petroleum Institute
FE	Finite Element
FFS	Fitness for Service
ID	Internal Diameter
OD	Outer Diameter
RP	Recommended Practice
SMSC	Stress-Modified Critical Strain
UTS	Ultimate Tensile Strength

CHAPTER 1

INTRODUCTION

1.1 PROJECT BACKGROUND

American Petroleum Institute (API) has classified the pipe for oil and gas. API X65 steel pipe is one of the pipes that is has been standardized by API and it was largely used in oil and gas industries. It was used as underground pipelines to transport the product of oil and gas. Underwater and underground position of the steel pipe makes it exposed to the salty environment and damp surrounding which can cause corrosion. During the installation of the pipelines, third party accidents could happen and caused dents and gouges to the pipelines due to contact of steel-steel and also minor scratches on the pipe. This thesis will apply the ductile failure criteria proposed by C.-K.Oh et al. (2007); on gouged API X65 steel pipes in terms of true fracture strain as a function to the stress triaxiality (defined by the ratio of the hydrostatic stress to the equivalent stress). To determine the true fracture strain of the pipe, a finite element (FE) modeling (MSC Patran 2008 r1) of smooth and gouged steel pipe with different gouge length are tested using FE analysis (MSC Marc). Simulation was made to emulate the variation of stress triaxiality of the ductile behavior on the material.

From the elastic-plastic deformation of the material, variation of stress triaxiality which leads to true fracture strains as a function of stress triaxiality can be obtained and used to determine the burst pressure of a gouged steel pipes. By applying this burst pressure equation, the stresses subjected to the material due to the internal pressure of the pipe and the other stresses involved on outer surface of the pipe can be determined.

But, in this thesis, the intention goes to the burst pressure of the API X65 steel pipes can withstand under the defective condition.

1.2 OBJECTIVES OF THE RESEARCH

The main objectives of this project are as follow:

1) To determine the burst pressure of defective API X65 steel pipes.

2) To investigate the effect of gouge length and pipe outer diameter on burst pressure.

1.3 SCOPE OF PROJECT

The scope of this project concentrates about the determination of burst pressure of defective steel pipes. API X65 steel pipes with the minimum specified yield strength and ultimate tensile strength are σ_y = 448 MPa and *UTS* = 530 MPa was used for subjecting the test of the burst pressure. The defect was interpreted as a gouge on the surface of the steel pipe. Different gouge length was studied to investigate its effect on the burst pressure of the steel pipes. MSC Patran/Marc was used for FE analysis to by applying the elasto-plastic isotropic homogeneous material model with reduced integration. A one-quarter model has been used to represent the full-scale model of the pipe for computational efficiency

1.4 PROBLEM STATEMENT

API X65 steel pipes is primarily used in the oil and gas industries. The ductility, high strength and low cost; makes it much more attractive than other type of steel pipe. Higher-performing steel was used since these industries routinely use miles of pipe. During the installation of the pipelines, defects are seldom happen which caused by the third party accidents such as dents and gouges. The pipeline was exposed to the environment salty sea water and makes it always exposed to the corrosive media. Corrosion happens, can cause the reduction in thickness of the pipe or in other words is called metal loss. Metal loss can be very dangerous to the pipeline and which could cause burst. For this thesis, metal loss from the pipe can be represented as a gouge on the surface of the pipe.

In order to maintain the integrity of the pipe, the burst pressure becomes the main parameter to be determined. The method to determine the burst pressure was by using FE analysis software. FE analysis was chosen rather than experimental analysis because experimental method is very complicated to be done. It requires some expensive equipment and material. Proper location of experiment is also need to be considered and it must be equipped with safety measures and acoustic proof, because the experiment will produce an explosion noise from the burst on the gouge. Using FE analysis, the test can be done with only by modeling and analyze the model.

CHAPTER 2

LITERATURE REVIEW

2.1 INTRODUCTION

A pipe is a tubular section or hollow cylinder, usually but not necessarily of circular cross-section, used mainly to convey substances which can flow — liquids and gases (fluids), slurries, powders, masses of small solids. It can also be used for structural applications; hollow pipe is far stiffer per unit weight than solid members. Pipes are utilized in various industries and applications. Such usages of steel pipes are for pipe pilling, road boring, floating docks, fencing, penstock, fiber-optics and drilling.

Some of oil pipeline applications are, oil pipeline API SPEC 5L for the purpose of transportation of gas, water, oil in oil & gas industry. API SPEC 5CT tubing is used in extracting petroleum & natural gas casing pipe serves as wall of well. ASTM A106 for the purpose of the pipeline project of boiler, water & petroleum. ASTM A53 it is used for conveying water, petroleum, gas and other common fluids. ASTM A179 for tubed heat exchanger and similar heat conveying equipments. ASTM A192 for manufacture wall panel, economizer, reheater, superheater and steam pipeline of boilers.

In oil and gas industry, most transportation of oil and as product uses a seamless steel pipes. Seamless steel pipes are a kind of hollow cross-section with no surrounding joints. It can be used for transmitting a large number of fluids such as oil, natural gas, water and some solid materials. At the same time it can be widely used as the manufacture of various structural parts and mechanical parts, such as the drill pipe, automotive transmission shaft, as well as building construction. Compared with the

solid steel such as round bar, at the same flexural torsional strength, the weight of Seamless steel pipe is lighter. It is a type of economic steel.

2.2 HISTORY

Fracture mechanics is a field of mechanics, concerned with the study of the propagation of cracks in materials. It uses methods of analytical solid mechanics to calculate the driving force on a crack and those of experimental solid mechanics to characterize the material's resistance to fracture. Most engineering materials were having ductile behavior, and shows some nonlinear elastic and inelastic deformation under operating conditions that involve larger loads. In such material, the assumptions of linear elastic fracture mechanics may not hold because of the plastic zone at a crack tip may have a size of the same order of magnitude as the crack size and the size and shape of the plastic zone may change as the applied force is increased and also as the crack length increases.

Therefore, a more general theory of crack growth is needed for elastic-plastic materials that can account for the local conditions for initial crack growth which includes the nucleation, growth and coalescence of voids or decohesion at the crack tip.

2.3 API 5L X65

API 5L X65 steel pipes was generally used as a medium to transport the hydrocarbon products from off-shore to on-shore or on the ground eventually. One interesting point is that, as most of the API X65 gas pipelines in Korea have been built within the last 10 years, mechanical properties of API X65 gas pipelines in Korea tend to have quite uniform properties (Oh C-K et al, 2007). Table 2.1 and 2.2 are the properties of API X65 steel pipe used in this thesis project.

Table 2.1: Chemical composition of the API X65 steel

Element (wt %)						
C	P	Mn	S	Si	F*e*	Ceq
0.08	0.019	1.45	0.03	0.31	Balance	0.32

Source: American Petroleum Institute (2000)

Table 2.2: Mechanical tensile properties at room temperature of the API X65 steel

Young's modulus *E (GPa)*	Poisson's Ratio *v*	Yield strength σ_y *(MPa)*	Tensile strength σ_u *(MPa)*
210.7	0.3	464.5	563.8

Source: American Petroleum Institute (2000)

2.4 TYPE OF DEFECTS ON STEEL PIPES

Oil and gas transmission pipelines have a good safety record and are a demonstrably safe means of transporting hydrocarbons. This is due to a combination of good design, materials and operating practices. However, like any engineering structure, pipelines do occasionally fail. The major causes of pipeline failures around the world are external interference and corrosion; therefore, assessment methods are needed to determine the severity of such defects when they are detected in pipelines (Cosham A, 2004). Assessment methods and determination of the burst pressure before a total lost could occur are needed to determine the rigorousness of such defects when they are detected in pipelines.

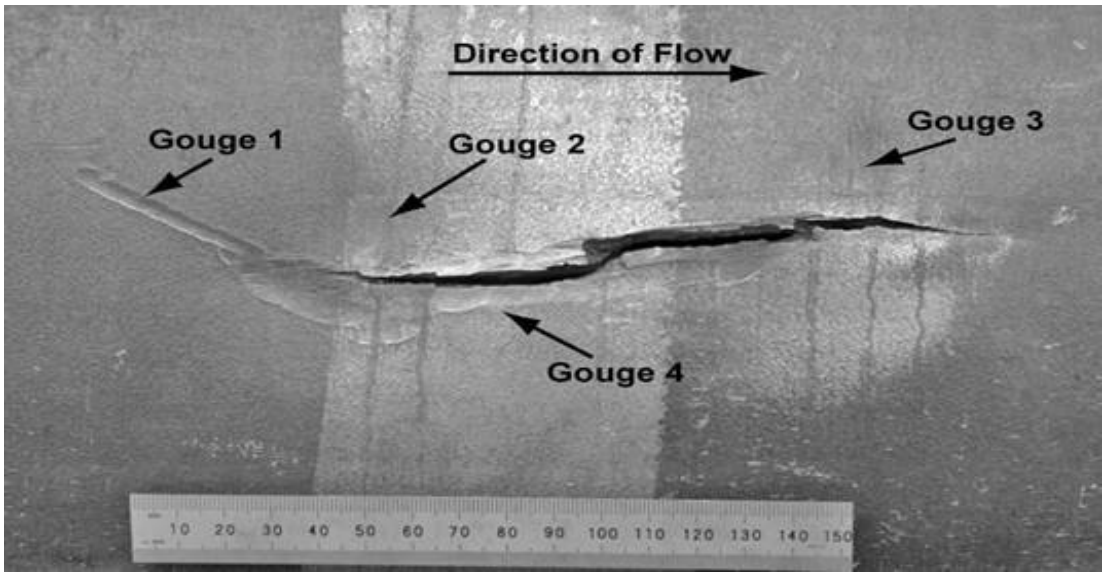

Figure 2.1: Gouged steel pipe

Source: Cosham A, 2004

2.4.1 Gouge

A gouge is defended as a type of chisel with a blade that has a concavo-convex section. Upon the corrosion process, metal loss from the steel pipe can occur and cause gouges on the outer surface or inner surface of the pipe. Because of the outer surface of the steel pipe is much exposed by the surrounding, the corrosion process are more likely to happen rather than the inner surface. As the gouges happen on the surface of the pipe, the wall thickness of the steel pipe could reduce and eventually cause in irregularity of the total shape of that particular pipe.

2.4.2 Dent

A dent in a pipeline is a permanent plastic deformation of the circular cross-section of the pipe and it is a gross distortion of the pipe cross-section (Cosham A and Hopkins P, 2004). Dent depth is defined as the maximum reduction in the diameter of the pipe compared to the original diameter. A dent would cause a local stress and strain concentration, and a local reduction in the pipe diameter. The dent depth is the most major factor affecting the burst strength and the fatigue life of a plain dent. The profile of the dent does not emerge to be a vital parameter, as long as the dent is smooth.

Whether a pipe is gouged during indentation depends on many factors, including the curve of the indentation, the frictional resistance between the surface of the pipe and the indenter, the shape and sharpness of the indenter, the pipe geometry, the material properties and the internal pressure. The stiffer the pipe, the more resistant it is to denting. Damage introduced into pressurized pipe tends to comprise shallower dents and deeper gouges than damage introduced into unpressurized pipe, because internal pressure stiffens the pipe. A sharp indenter is more likely to cut into the pipe wall when the pipe is pressurized. Experimentally it has been observed that coated and lubricated pipe surfaces prolong less damage than do dry, bare pipe surfaces.

2.4.3 Corrosion

Corrosion is an electrochemical process. It is a time dependent mechanism and depends on the local environment within or adjacent to the pipeline. Corrosion usual

appears as either general corrosion or localized (pitting) corrosion. There are many different types of corrosion, including galvanic corrosion, microbiologically induced corrosion, AC corrosion, differential soils, differential aeration and cracking. Corrosion causes metal loss.

Corrosion in a pipeline may be difficult to characterize. Typically, it will have an irregular depth profile and extend in irregular pattern in both longitudinal and circumferential directions. It may occur as a single defect or as a cluster of adjacent defects separated by full thickness (un-corroded) material. There are no clear definitions of different types of corrosion defects. The simplest and perhaps most widely recognized definitions are as follows: pitting corrosion, defined as corrosion with a length and width less than or equal to three times the un-corroded wall thickness, and general corrosion, defined as corrosion with a length and width greater than three times the un-corroded wall thickness.

2.5 STRESSES ACTED ON STEEL PIPES

A broadly accepted method of predicting tubing failure due to pressure and tension limits is based on the von Mises stress. If the von Mises stress exceeds the yield strength of the material, the tubing is assumed to fail. The von Mises stress is a combination of the three principal stresses in and the shear stress caused by torque. The three principal stresses are axial stress (σ_a), radial stress (σ_r) and Tangential or hoop stress (σ_h). There are two types of assumptions made in analyzing these principle stresses. Those are thin-walled pressure vessel and thick walled pressure vessels. Thin-walled pressure vessel can be assumed when the ratio of $\frac{r}{t} \geq 10$. Generally, a pressure vessel is considered to be thin-walled if its radius, *r* is larger or equal than 10 times its wall thickness, *t*. On the other hand, it was assumed that for thick-walled pressure vessel must have a ratio of $\frac{r}{t} \leq 10$. That means the pressure vessel is considered to be thin-walled if its radius, *r* is smaller or equal than 10 times its wall thickness, *t*.

The coordinates used to describe the cylindrical vessel can take advantage of its axial symmetry. It is natural to align one coordinate along the axis of the vessel in the longitudinal direction). To analyze the stress state in the vessel wall, a second coordinate is then aligned along the hoop direction. With this choice of axisymmetric

coordinates, there is no shear stress. The hoop stress σ_h and the longitudinal stress σ_l are the principal stresses.

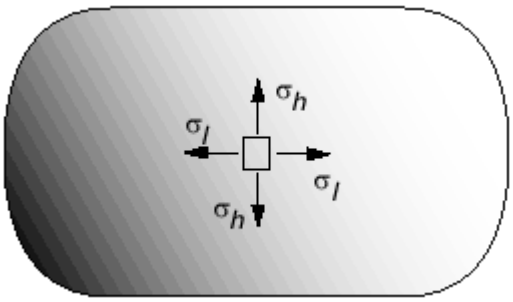

Figure 2.2: Direction of hoop and longitudinal stress

Source: Beer FP, Jr. Johnston ER, De Wolf JT (2006)

2.5.1 Hoop Stress

A circumferential stress which, in a pipe or pressure vessel would tend to make the pipe diameter or circumference increases. As fluid which has filled the pipe is pressurized the hoop stress causes the diameter or circumference to increase. The force resisted by the tangential stress can be called as *hoop stress* and it is acting uniformly over the stressed area for thin-walled pressure vessel. The free body is in static equilibrium. According to Newton's first law of motion, the hoop stress yields;

$$2 \cdot \sigma_h \cdot t \cdot dx = p \cdot 2 \cdot r \cdot dx \tag{2.1}$$

$$\sigma_h = \frac{pr}{t} \tag{2.2}$$

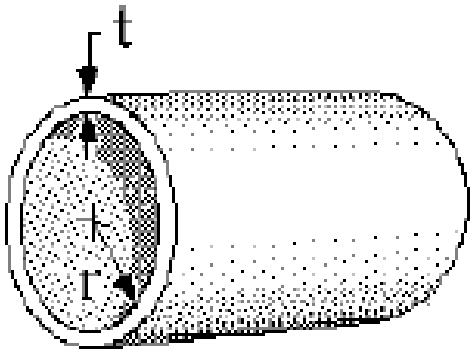

Figure 2.3: Ratio of pipe radius to pipe thickness

Source: Beer FP, Jr. Johnston ER, De Wolf JT (2006)

But, if the cylindrical pipe or pressure vessel has a ratio of $\frac{r}{t} \leq 10$, the cylinder can be considered as a thick-walled vessel and the hoop stress of the cylinder is equal to the tangential stress;

$$\sigma_t = \left[\frac{(p_i r_i^2 - p_o r_o^2)}{r_o^2 - r_i^2}\right] - \left[\frac{r_o^2 r_i^2 (p_o - p_i)}{r^2 (r_o^2 - r_i^2)}\right] \tag{2.3}$$

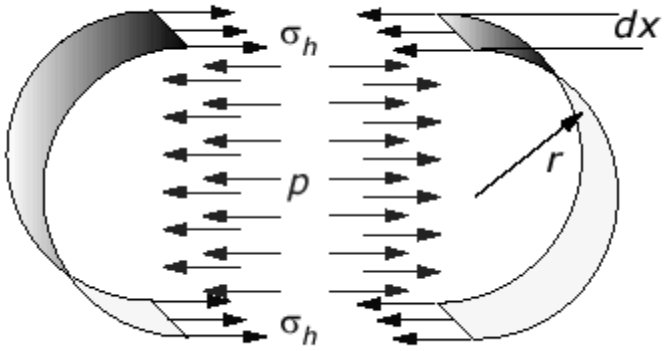

Figure 2.4: Hoop stress acted on steel pipe

Source: Beer FP, Jr. Johnston ER, De Wolf JT (2006)

2.5.2 Radial Stress

When the assumption for thin wall states that if $\frac{r}{t} \geq 10$, the ratio of the internal radius of the pipe and the thickness is less than 10. The stress acted on the z axis is equal to zero (0), $\sigma_z = 0$, and thus the radial stress σ_r will also equal to zero $\sigma_r = 0$ because the radial stress acted on the pipe is rotated along the z-axis.

2.5.3 Axial Stress

Defined as, the tension or compression stress created in a structural member by the application of a lengthwise axial load. Sometimes, axial stress also called as longitudinal stress.

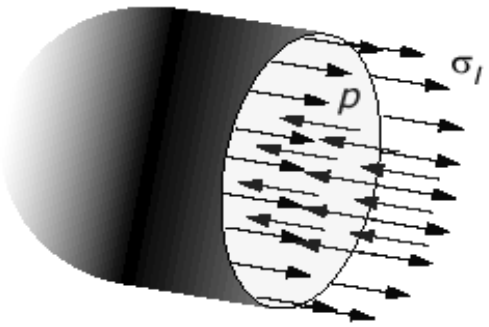

Figure 2.5: Longitudinal stress acted on steel pipe

Source: Beer FP, Jr. Johnston ER, De Wolf JT (2006)

To determine the longitudinal stress σ_l, we make a cut across the cylinder similar to analyzing the spherical pressure vessel. The free body, illustrated on the above, is in static equilibrium. This implies that the stress around the wall must have a resultant to balance the internal pressure across the cross-section.

Applying Newton's first law of motion, we have,

$$\sigma_l \cdot t \cdot 2\pi r = p \cdot \pi r^2 \quad (2.4)$$

$$\sigma_l = \frac{pr}{2t} \tag{2.5}$$

The equation stated above can only be used if the pipe or pressure vessel is assumed as a thin-walled.

2.5.4 Burst Pressure of a Pipe

Burst pressure for direct definition is; maximum pressure. To be general, a defective pipe would have a lower burst pressure rather than a non-defective pipe. To be précised, it is a pressure limitation of a pipe can withstand before it damage/defective (without bursting). Burst pressure can be calculated by using Barlow's Formula.

$$P = \frac{2\,s\,t}{d_0\,SF} \tag{2.6}$$

With, s, for the material strength (MPa), t, wall thickness of pipe, d_0, is the outer diameter of the steel pipe, and SF, is the safety factor of the material which is usually 1.5 to 10. Equation (2.6) is based on ideal condition at room temperature with no defect on the pipe outer surface. Thus, ultimate tensile strength can be used to determine the bursting pressure and yield strength can be used at which the permanent deformation of the material begins.

2.6 THEORY

After all, the stresses acted on the steel pipe could not be determined by using the equations of hoop, radial and axial stress because the pipe has been gouged as a substitute to the defect on a steel pipe. Those stresses only applicable, if the pipe used was free of defects. In this analysis of determining the burst pressure of defective steel pipe, the Stress Modified Critical Strain (SMSC) approach was used, because it is more fundamental. SMSC approach was based on the analysis of the 'local' criterion. Noting that the process of ductile fracture involves void nucleation, growth and coalescence and it is strongly dependent on the hydrostatic stress state (Oh CK, Kim YJ, Baek JH, Kim WS, 2007). Failure initiates in the central region of the gouge where the stress state is most severe and different stress states can be obtained with gouge of different severity

and depth (McClintock FA, 1968). When fully plastic conditions are reached, stress and strain in the failure region can be estimated. SMSC model consist not only of mechanical parameters such as stress and strains, but also of material parameters that are constant and might be related to metallurgy. These material constants are typically regarded as material properties and thus should be calibrated for given material. With these material constants, and modified strain approach can be applied to predict the ductile fracture of defective structures. This thesis will present the SMSC for API X65 Steel Pipe, as a function of the stress triaxiality.

2.6.1 Stress-Strain Curve

During tensile testing of a material sample, the stress–strain curve is a graphical representation of the relationship between stress, derived from measuring the load applied on the sample, and strain, derived from measuring the deformation of the sample, i.e. elongation, compression, or distortion (Roylance D, 2001). The slope of stress-strain curve at any point is called the tangent modulus; the slope of the elastic (linear) portion of the curve is a property used to characterize materials and is known as the Young's modulus.

Suppose that a metal specimen be placed in tension-compression-testing machine. As the axial load is gradually increased in increments, the total elongation over the gauge length is measured at each increment of the load and this is continued until failure of the specimen takes place. Knowing the original cross-sectional area and length of the specimen, the normal stress σ and the strain ε can be obtained. The graph of these quantities with the stress σ along the y-axis and the strain ε along the x-axis is called the stress-strain diagram. The stress-strain diagram differs in form for various materials. The diagram shown below is that for a medium-carbon structural steel.

Metallic engineering materials are classified as either ductile or brittle materials. A ductile material is one having relatively large tensile strains up to the point of rupture like structural steel and aluminum, whereas brittle materials has a relatively small strain up to the point of rupture like cast iron and concrete. An arbitrary strain of 0.05 is frequently taken as the dividing line between these two classes.

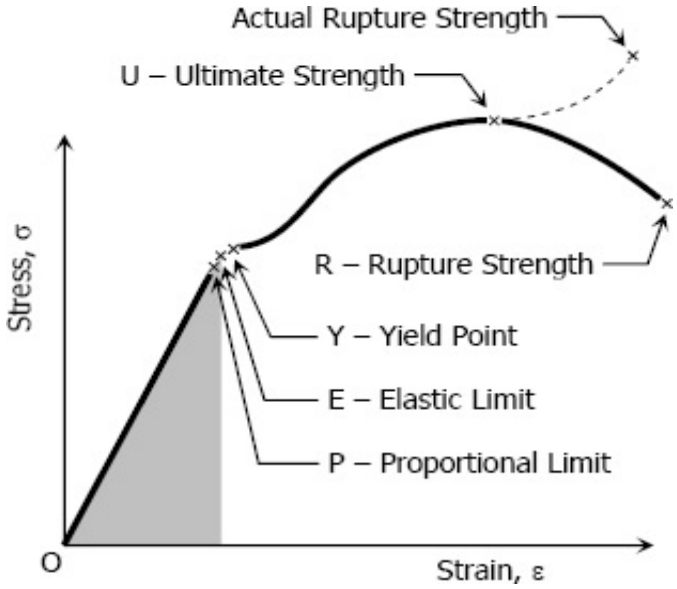

Figure 2.6: Stress-strain curve of a ductile material

Source: Roylance (2001)

2.6.2 Yield Stress

Yield strength is a very important value for use in engineering structural design. If we are designing a component that must support a force during use, we must be sure that the component does not plastically deform. Structural elements and machine components made of a ductile material are usually designed so that the material will not yield under the expected loading/pressure conditions. When element or component is under uniaxial stress, the value of the normal stress, $\sigma_{x,}$ which will cause the material to yield, can be obtained readily from the tensile test conducted on a specimen of the same material. Thus, we can state that the element or component will be safe as long as $\sigma_x < \sigma_y$, where σ_y is the yield strength of the test specimen.

2.6.3 Maximum-Shearing-Stress Theory vs. Maximum-Distortion-Energy Theory

Maximum-Shearing-Stress (MSS) Theory is based on the observation that yield in ductile materials is caused by slippage of the material along oblique surfaces and is due primarily to shearing stresses (Beer FP, 2006). According to this criterion, a given structural component is safe as long as the maximum value τ_{max} of the shearing stress in that component remains smaller than the corresponding value of the shearing stress in a tensile test specimen of the same material as the specimen starts to yield.

With respect to 2D stress, the maximum shear stress is related to the difference in the two principal stresses. Therefore, the criterion requires the principal stress difference, along with the principal stresses themselves, to be less than the yield shear stress.

$$|\sigma_1| \leq \sigma_y$$

$$|\sigma_2| \leq \sigma_y$$

and

$$|\sigma_1 - \sigma_2| \leq \sigma_y \tag{2.7}$$

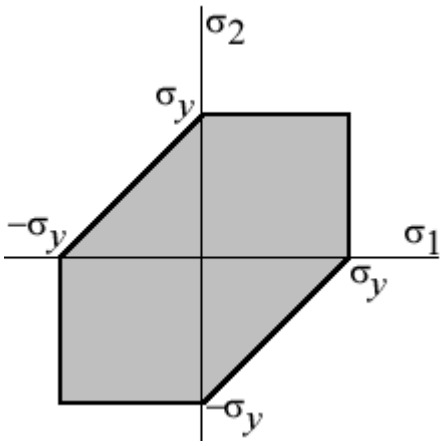

Figure 2.7: Tresca diagram

Source: Nisbett KJ (2009)

According to the von Mises criterion, after the German-American applied mathematician Richard von Mises (1883-1953), states that the failure occurs when the energy of distortion reaches the same energy for yield/failure in uniaxial tension. A given structural components is safe as long as the maximum value of the distortion energy per unit volume in the material remain smaller than the distortion energy per unit volume required to cause the yield in a tensile test specimen of the same material (Beer FP, 2006). Mathematically, this is expressed as

$$\frac{1}{2}[(\sigma_1 - \sigma_2)^2 + (\sigma_2 - \sigma_3)^2 + (\sigma_3 - \sigma_1)^2] \leq \sigma_y^2$$

In the cases of plane stress, $\sigma_3 = 0$. The von Mises criterion reduces to

$$\sigma_1^2 - \sigma_1\sigma_2 + \sigma_2^2 \leq \sigma_y^2 \quad (2.8)$$

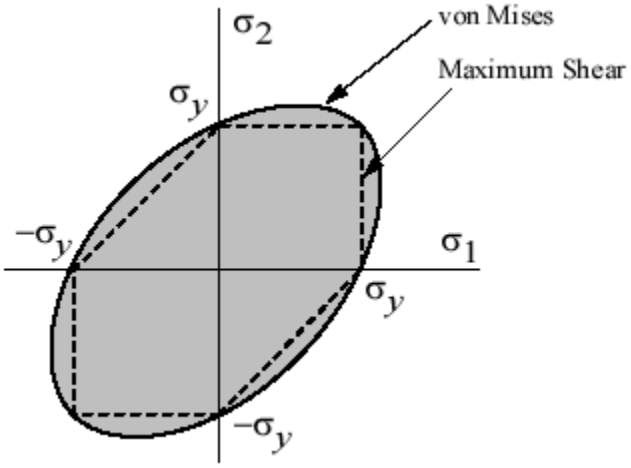

Figure 2.8: Distortion energy diagram

Source: Nisbett KJ (2009)

Since the values of the yield strength σy in tension and of the yield strength τy in shear are given for various ductile materials, we can compute the ratio of $\frac{\tau_y}{\sigma_y}$ for the material and verify that the values obtained range from 0.55 to 0.60. Thus, the maximum distortion energy theory appears somewhat more conservative than the maximum shearing stress theory as far as predicting yield in torsion is concerned.

In this thesis, the distortion energy theory could not be used because the von Mises theory was made to determine the stress on the unflawed material. Under the circumstances of a gouged pipe, a more discreet theory need to use and a specific equation to determine the fracture strain on the defect area. When the failure pressure was normalized by the FE obtained for unflawed pipe under various flaw and pipe configuration, the failure pressure of carbon steel was almost lower Kamaya M, 2008). The existing assessment criteria developed for line pipe steel can be applied to make a conservative assessment of carbon steel.

2.7 STRESS-MODIFIED CRITICAL STRAIN

2.7.1 Stress Triaxiality Variations

The distortion energy theory predicts that the yielding occurs when the distortion strain energy per unit volume reaches or exceeds the distortion strain energy per unit volume for yield in simple tension or compression of the same material (Budynas RG, 2008). The distortion energy theory originated from the observation that ductile materials stressed hydrostatically exhibited yield strengths greatly in excess of the values given by the simple tension test. Therefore, it was populated that yielding was not a simple tensile or compressive phenomenon at all, but rather that it was related somehow to the angular distortion of the stressed element. To develop the theory, the unit volume subjected to any three-dimensional stress state designated by the stresses σ_1, σ_2 and σ_3.

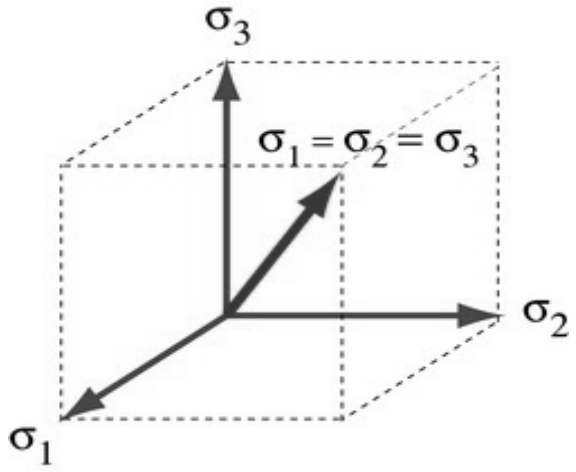

Figure 2.9: Principle stresses acted at a point

Source: Nisbett KJ (2009)

The stresses that undergone the hydrostatic tension due to σ_{ave}, acting in each of the same principle direction as shown in Figure 2.9. Thus,

$$\sigma_{ave} = \frac{\sigma_1 + \sigma_2 + \sigma_3}{3} \tag{2.9}$$

Stress triaxiality is defined by the ratio of the hydrostatic stress, σ_m, to the equivalent stress, σ_e :

$$\frac{\sigma_m}{\sigma_e} = \frac{\sigma_1 + \sigma_2 + \sigma_3}{3\sigma_e} \tag{2.10}$$

Where, σ_1, σ_2 and $\sigma 3$ are the principle stresses on the material. Stress triaxiality can be expressed in terms of three principle stresses as:

$$\sigma_e = \frac{1}{\sqrt{2}}\left[(\sigma_1-\sigma_2)^2 + (\sigma_1-\sigma_3)^2 + (\sigma_3-\sigma_2)^2 \right]^{0.5} \tag{2.11}$$

The equivalent strain of the material will defined by

$$\varepsilon_e = \frac{\sqrt{2}}{3} [(\varepsilon_1-\varepsilon_2)^2 + (\varepsilon_1-\varepsilon_3)^2 + (\varepsilon_3-\varepsilon_2)^2]^{0.5} \tag{2.12}$$

2.7.2 Stress-Modified Fracture Strain

By combining such information of detailed elastic-plastic analysis FE analyses with the large geometry change option of a notched bar tensile test, accurate values of stress and strain components can be determined at every stage of deformation. A ductile failure criterion in terms of equivalent strain to failure as a function to stress triaxiality can be established. The stress and strain only defined at a specific point where failure is most likely to start, corresponding to the place with highest stress triaxiality and strain or with the highest damage.

True fracture strain for critical location approach can be defined as exponentially dependent on the stress triaxiality (Rice and Tracey, 1969).

$$\varepsilon_{ef} = 3.29 \exp\left(-1.54 \frac{\sigma_m}{\sigma_e}\right) + 0.10 \tag{2.13}$$

CHAPTER 3

METHODOLOGY

3.1 INTRODUCTION

This chapter presents the overall methodology involved on the computer simulation process of this thesis. Research methodology describes the type of this thesis, scope of work, detail process of the project, assumptions made, and the scope of output. Those procedures involved, several problems encountered within this project and the experimental methods will be discussed clearly step by step throughout this chapter.

These methodologies can be described as the framework of the research where it contains the elements of work based on the objectives and scopes of the research. This chapter was intended to elaborate about the simulation under some circumstances conditions.

3.2 PROJECT FLOWCHART

The sequence of work represent in form of flowchart that has been planned is shown in the Figure 3.1 below. This flowchart is useful as a guideline to ensure that the simulation is carried out smoothly. The process involved in this project flowchart will be the limited to validation of burst pressure result analysis of defective steel pipe from previous peer researchers and Parametric Studies of this project under the guidelines of the objectives and scopes of study.

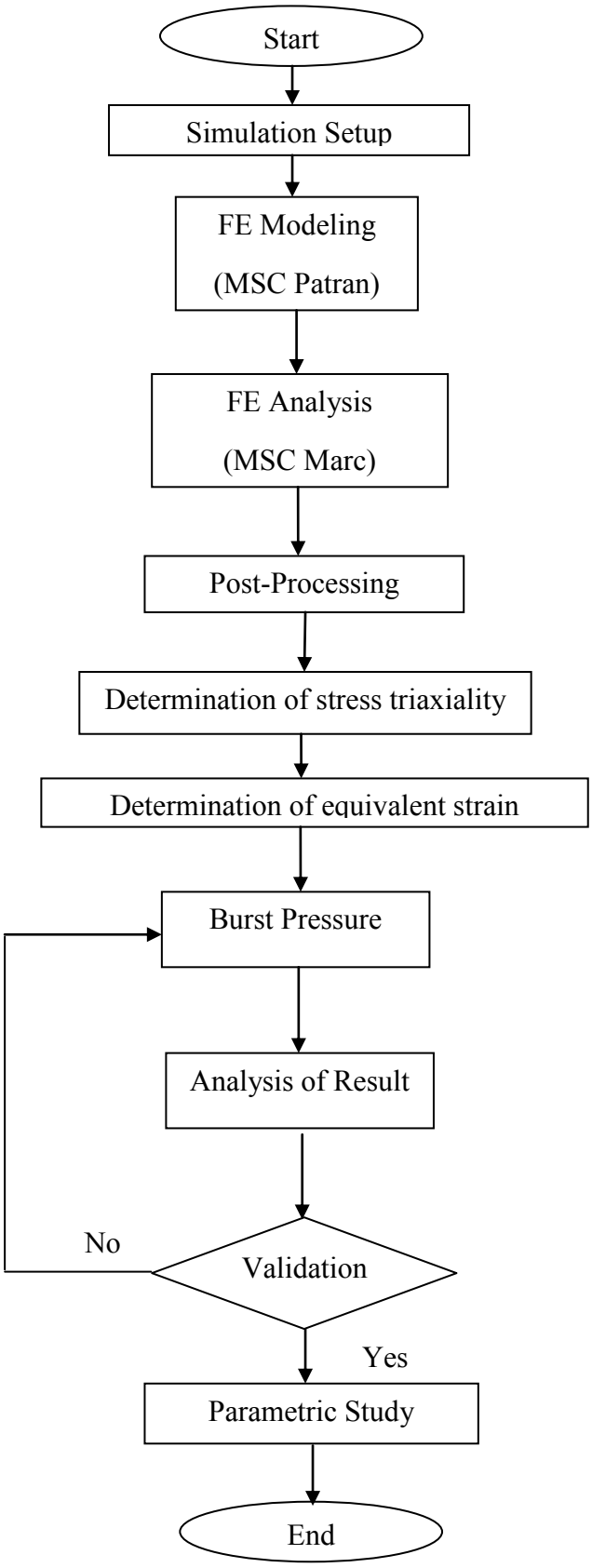

Figure 3.1: Project Flowchart

3.3 TYPE OF PROJECT

In this project, a computer simulation was used to determine the burst pressure of the defective steel pipe. This was done to validate the previous peer researcher's results and also the parametric studies for this project. MSC Patran 2008 r1 was used as a tool to model the API X65 steel pipes by fully applies symmetrical condition and also several parameters of the pipe. MSC Marc was used to analyze the steel pipe as an analysis tool. MSC Marc allows the user to perform a wide variety of structural, thermal, fluid and coupled analyses using the finite element method. These procedures provide solutions for simple to complex linear and nonlinear engineering problems. MSC Marc was chosen as a solver because it offers a vast selection of element types, material models, analysis capabilities, automated contact procedures and adaptive meshing.

3.4 SCOPE OF WORK

The work related to make this project become true is to identify the problem encountered in the real world and to initiate a test with the computer simulation. Especially when it comes to identifying the limitation of pressure that a defect oil and gas pipe line before it will burst. Thus, the objective of this project will be the measures, limitations and guidelines to embrace the burst pressure of the defective steel pipe.

By developing and designing the criteria of a pipe in MSC Patran, the simulation can be run by using MSC Marc as the solver to solve the equation and problem related to elastic-plastic deformation until the gouged pipe reached the fracture point. After the simulation ran, all data principle stresses (for each particular time) by the solver was extracted and transferred to Microsoft Office Excel to calculate the equivalent stress and equivalent strain. At the end of analysis using Microsoft Office Excel, the burst pressure can be identified when the equivalent strain is more than the fracture strain.

For validation part, the results from FE analysis will be compared to the experimental data by previous researcher (Chang et al, 2007). Then, as to complete the

objectives of the study, some parameter such as the outer diameter, *OD* and the gouge length, *l* will be varied.

3.5 PIPE MODELLING

In this project, a pipe model was made as a one-quarter symmetrical test for the computer simulation. The pipe has the diameter of, *OD* = 762 mm, the thickness of, *t* = 17.5 mm, and the total length of, *L* = 2300 mm. The gouge is located at the center of the pipe and characterized by the 45 degree V- notch with the circular radius of 2mm. The depth of the gouge is *d* = 8.75 mm which is 50 percent of the pipe thickness, *d/t* = 0.5. Figure 3.2 shows the illustration of the defective pipe.

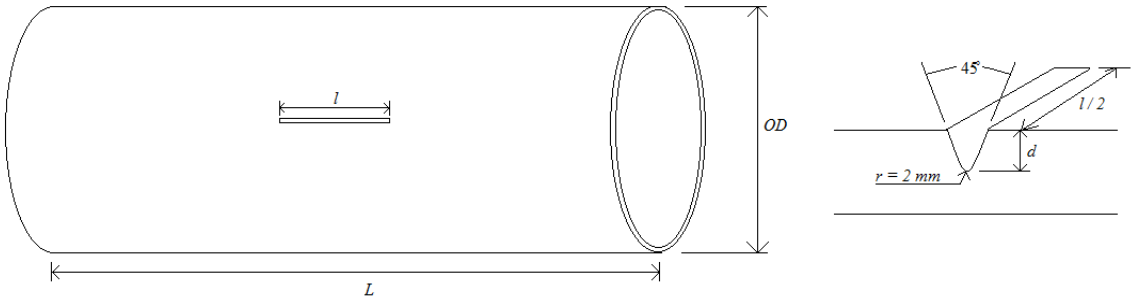

Figure 3.2: Illustration of defective pipe

3.5.1 Outline of the pipe

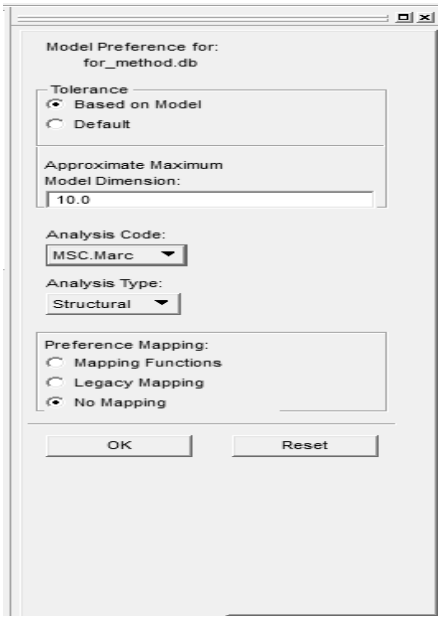

Figure 3.3: Solver options

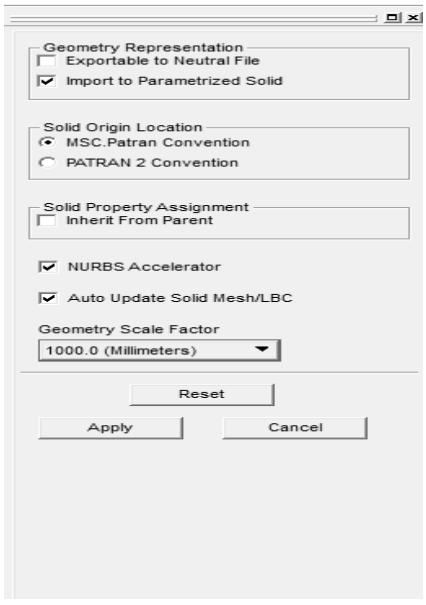

Figure 3.4: Geometry dimension option

Figure 3.3 and 3.4, show the initial setup before run the simulation. It is essential to set the solver (analysis code) that needed to be used and also the overall of the model units (geometry scale factor).

The pipe was drawn as the figure below;

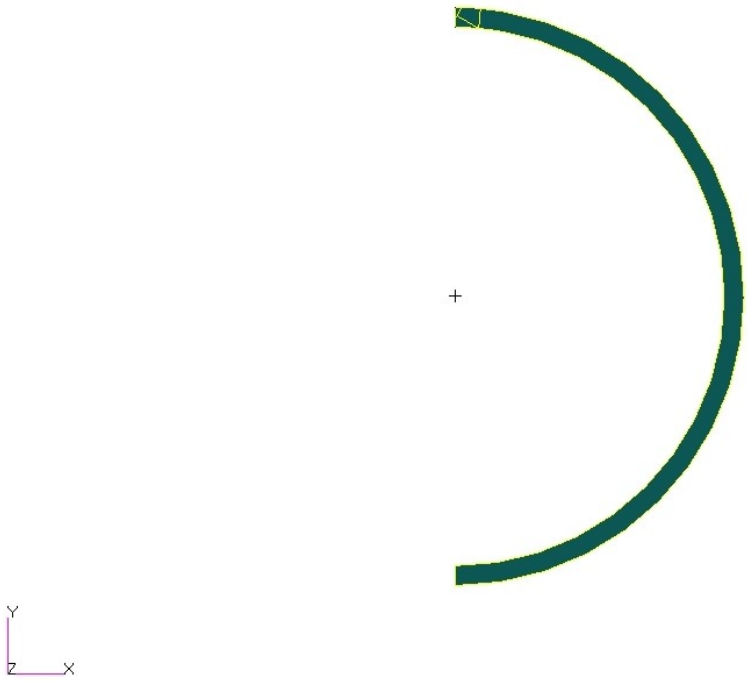

Figure 3.5: Initial pipe surface

Figure 3.5 shows the initial pipe surface made in MSC Patran. After the outline of the pipe was done, surfacing all of the inner face of the pipe was done. It is important to make sure that the direction of the surface is directed to the positive of z-axis all of the direction of the surface are the same. To check the surface either it is normal or not, is to show the customariness of the surface. If the surface is not normal, the surface can be reverse and vice-versa.

3.5.2 Pipe modeling

The previous outline of the pipe would now be extruded to make it a solid surface. According to the initial dimension of the pipe, the initial pipe length, L_0 is 2300 mm. Table 3.1 indicates the dimensions of the full-scale pipe model with gouge defect.

Table 3.1: Dimensions of the full-scale pipe model with gouge

Pipe number	**Length, *L* (mm)**	**Diameter, *D* (mm)**	**Thickness, *t* (mm)**	**Gouge depth, *d* (mm)**	***d/t***	**Gouge length, *l***
A B	2300	762	17.5	8.75	0.5	100 200

Figure 3.6 shows the model sample used in this analysis, axis-symmetry was been taken into a count and make the pipe length to 1150 mm. Because there was a 100 mm gouge - as a defect alternate – was made on the pipe, the outline was extruded 50 mm to the front (positive z-axis) and 1100 mm to the back of the outline (negative z-axis). Beneath, is the figure of the modeled steel pipe.

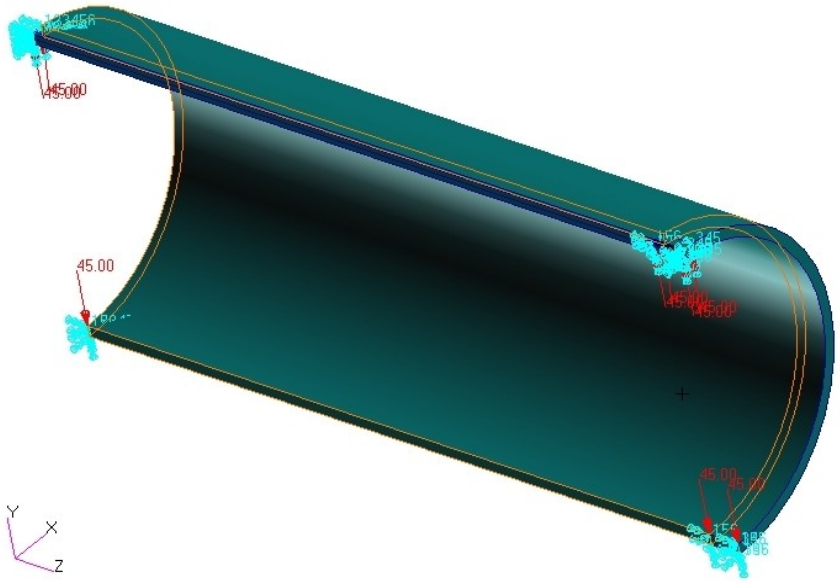

Figure 3.6: Symmetrical pipe model

3.5.3 FE meshing on pipe model

To form the mesh on the pipe model, mesh seed was added at the pipe curves. Type of mesh distribution used was one way bias. One way bias type was used for the reason that the meshes must be very small at the critical point, where the burst could take place on the pipe.

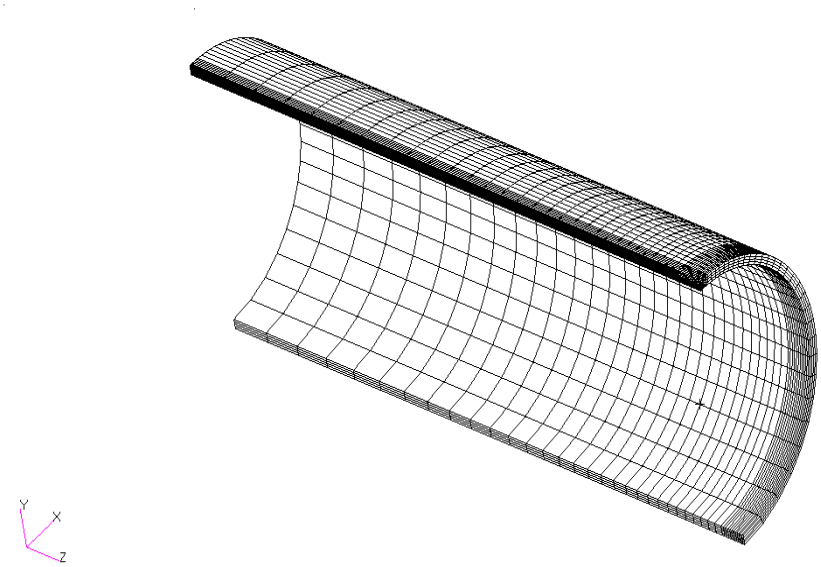

Figure 3.7: Detail meshing on the pipe

The centre of gouged surface was identified as the place that the fracture of the pipe could likely happen. So, much less significant mesh was allocated at that surface as at that point, because the stress-strain would be the highest among all. Figure 3.7 and 3.8 shows detailed image of FE meshing on gouged pipe model. The meshing on gouge area were made to finer element size to have a close to accurate value calculation for stress acted at the area.

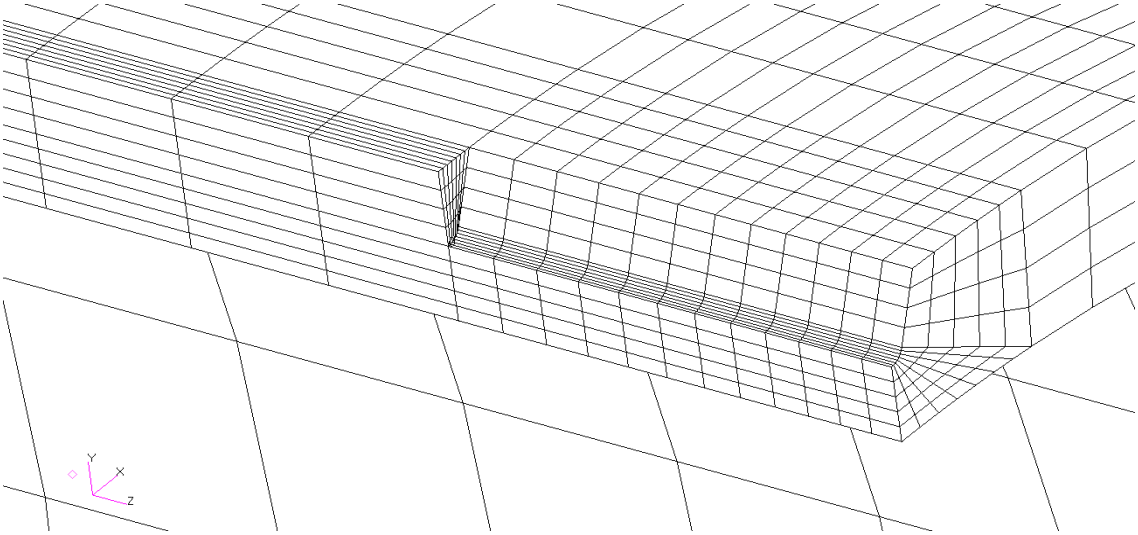

Figure 3.8: Detailed meshing on the gouge defect

3.5.4 Boundary conditions and internal pressure

The boundary condition was applied at the end of the pipe as a fixed. According to the full-scale pipe model experiment, the end of both side of the pipe was welded with a cap to allow the pressure applied inside the pipe.

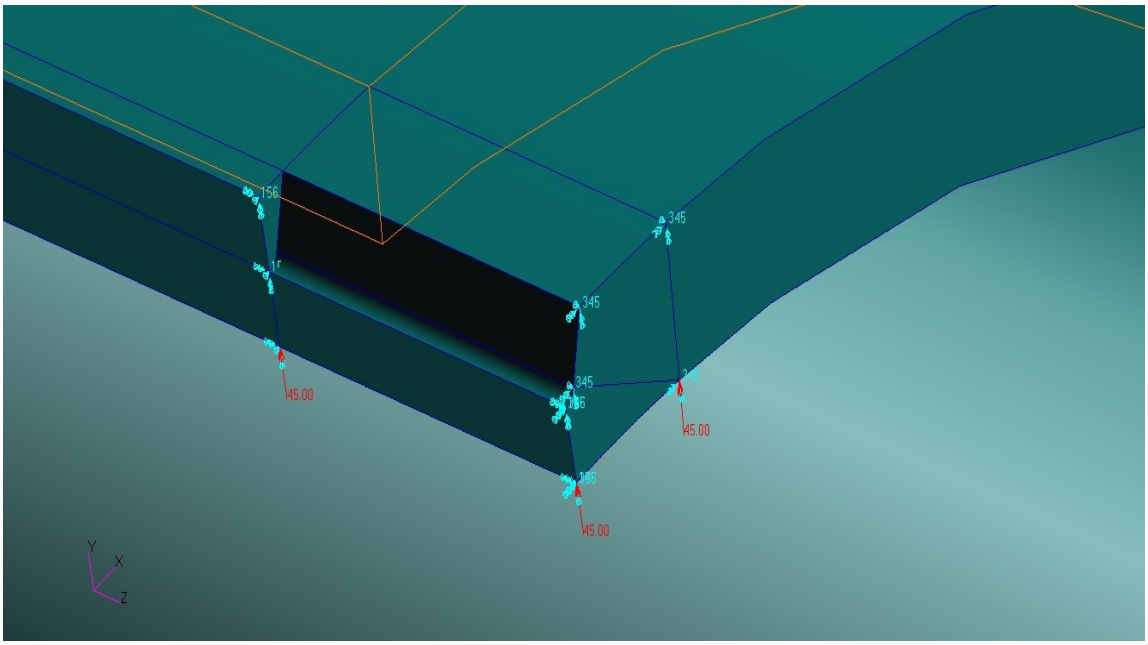

Figure 3.9: Boundary conditions and internal pressure

Figure 3.9 shows the additional half diameter of the pipe was noted as the x-symmetry boundary conditions and another half length of the pipe was noted as the z-symmetry boundary condition. Thus, this analysis only requires quarter of pipe model. By this, it will utilize us to have more easy way to design the outline of the pipe and also to apply the pressure acted on the internal surface of the pipe.

For the internal pressure within the pipe, a pressure of 30 MPa was applied to the internal face of the pipe. This pressure was considered after the burst pressure determined of Oh CK (2007) work as a he had the burst pressure within the range of 22.48 MPa till 24.68 MPa for the experimental test of the unrestrained pipe.

3.5.5 Material properties

Figure 3.10 shows the process of assigning material properties for the model of both elastic and plastic behavior.

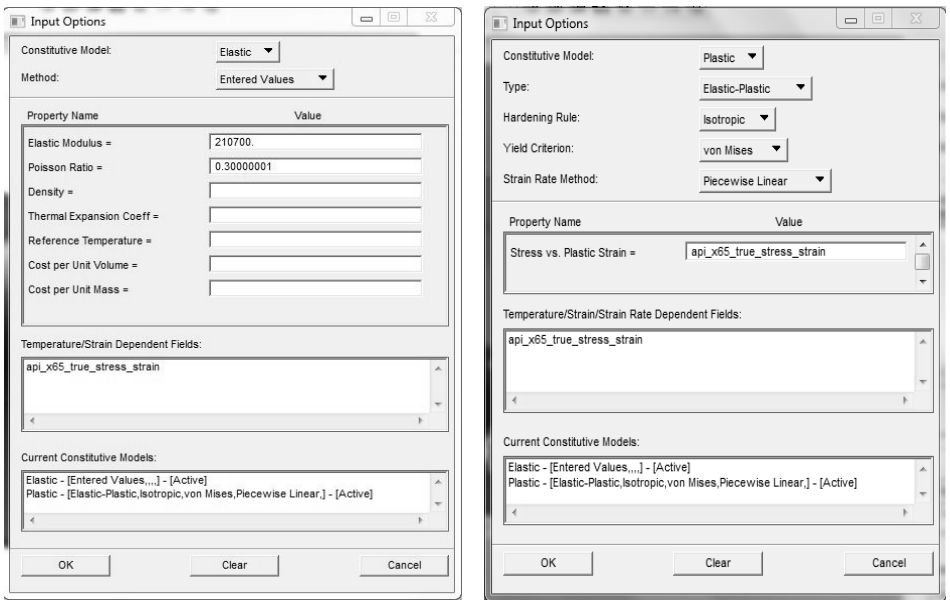

Figure 3.10: Material properties of the model for elastic and plastic

As stated previously, the Young's Modulus for API X65 Steel Pipe was 210.7 GPa and the Poisson's ratio is 0.3 for elastic properties. At plastic region, the detailed elastic-plastic data was keyed in the field area and inserted into the material properties.

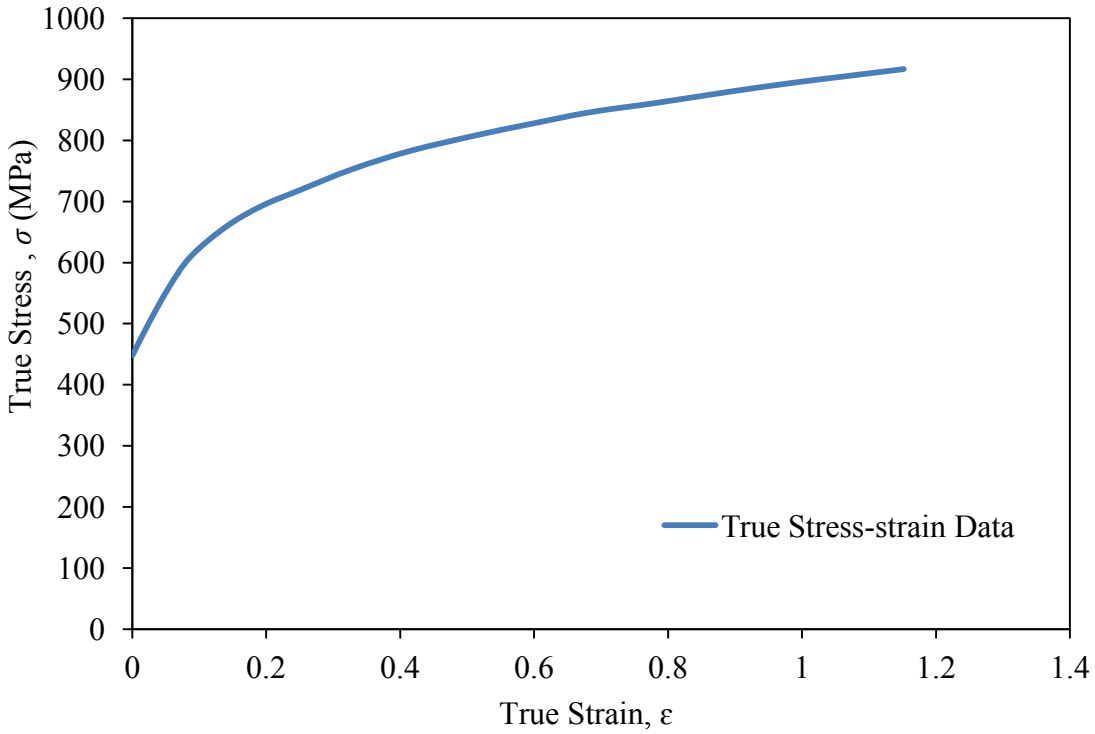

Figure 3.11: True stress-strain data for API X65 steel pipes

The values as in Figure 3.11 were extracted using Engauge software and the values was entered in the input option of the material properties, as seen in Figure 3.10. The constitutive model was modeled as an isotropic elastic-plastic material that obeys the incremental of plasticity theory. So that the solver would know that the material has a ductile behavior.

After completing the input of material properties, then, applying the properties to the model was made. By select application region, whole model can apply with the properties keyed in as in Figure 3.12.

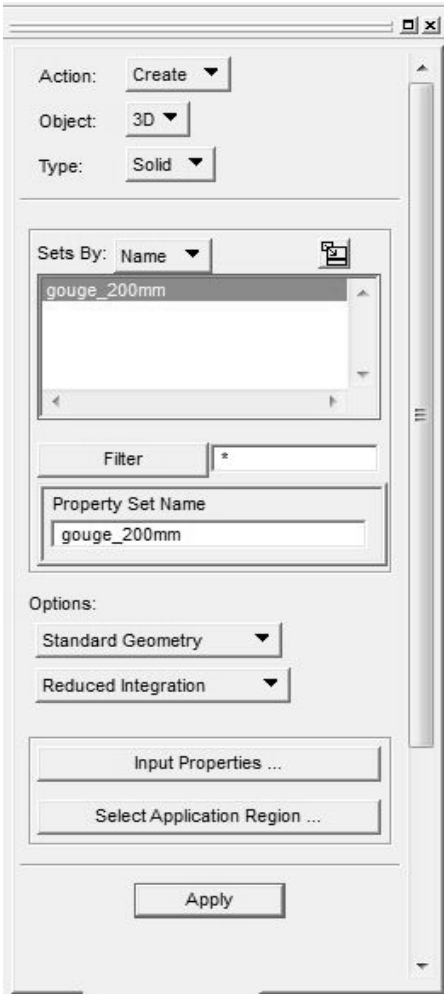

Figure 3.12: Model meshing type and properties

Reduced Integration was chosen as the formulae to be applied in the material properties. Reduced Integration is the simplest way to avoid locking. The basic idea is simple: since the fully integrated elements cannot make the strain field volume preserving at all the integration points, it is tempting to reduce the number of integration points so that the constraint can be met. Reduced integration usually means that the element stiffness is integrated using an integration scheme that is one order less accurate than the standard scheme. To set the true stress-strain data for API X65, Figure 3.13 shows how the method can be made.

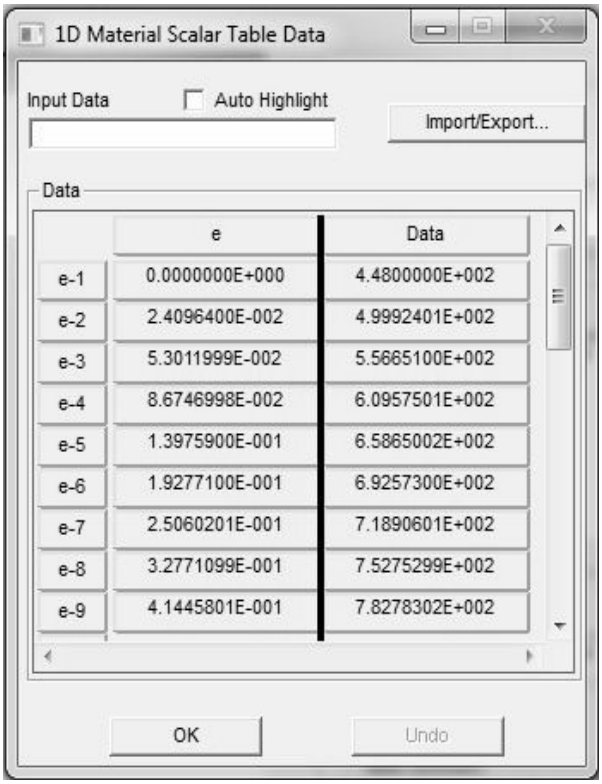

Figure 3.13: True stress-strain values for API X65

The true stress-strain data for API X65 was imported into MSC Patran, as seen in Figure 3.13. Thus, those data was then applied to the analysis so that the solver may know what the value of true stress and true strain of the model as simulation is running for analysis.

3.6 SIMULATION PROCEDURES

One reason for the failure of fracture mechanics, is to rectify the tunnel lies in the lack of a justified methodology to transfer material properties measures in standard laboratory specimens to large, complex flawed structures. Specifically, the use of toughness measured in deep, through-cracked, bend fracture specimens to predict the behavior of shallow, part-through cracks in a structure loaded primarily in tension, in many cases leads to uncertainties in assessment of fitness-for-purpose and remaining highly constrained specimen geometries generally provide conservative measurement of toughness, and as such do not produce accurate assessment for less constrained structures. The conservatism that is introduced may result in unnecessary and costly

repairs or in the removal from service of an important facility, with a corresponding loss of confidence in fracture mechanics analyses.

The effect of the constraint can be eliminated as an explicit issue by testing actual structural configurations or by matching the constraint of a laboratory specimen to that of the structure; however, such an approach is not straightforward and can be prohibitively costly. The recognition that constraint influences the driving force for fracture rather than the material resistance to fracture (toughness) has led to the formalization of methodology to quantify constraint effects through fracture model coupled with finite element generated crack tip stress strain field. In these methodologies, the models identify the local conditions at fracture initiations using crack tip stress strain. Finite element analysis is used to predict the influence of specimen geometry, loading mode and material flow properties on the crack tip fields. The value of the global parameter associated with satisfying the local conditions needed for fracture initiation is said to be critical value specific to the particular geometry analyzed. Repeating this type of analysis for a variety of specimens allows for trends in the variation of the critical global parameter due to size, geometry and loading to be defined. Constraint corrections can then be made to the critical global parameter obtained in toughness testing of standard laboratory specimens.

3.6.1 Analysis of the pipe model

When the result has obtained after the analysis of the model was complete and the result of the displacement of the gouge, the data of the local maximum principle stress, medium principle stress and minimum principle stress in the minimum section can be extracted from the FE results, as a function of the applied internal pressure. Those principle stresses can be used as the σ_1, σ_2 and σ_3 in calculating the equivalent stress. Same goes to the values of strain, as those principle stresses ε_1, ε_2 and ε_3 can be obtained by the value of maximum, medium and minimum principle stresses of the model. Figure 3.14 shows how values of principle stresses and strains of principle stresses and strain can be obtain.

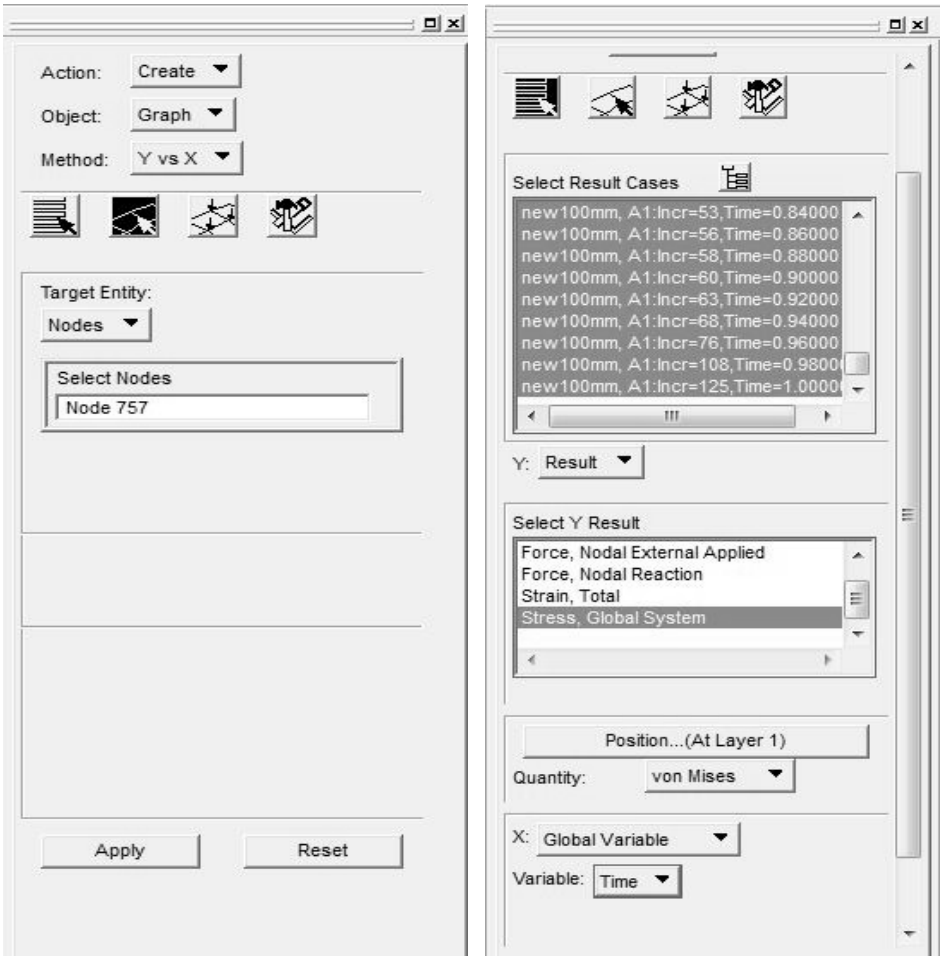

Figure 3.14: Values of principle stresses and strains

3.6.2 Determining the burst pressure

As the value of the principle stresses and principle strain obtained from the result of the analysis, the burst pressure of the pipe can merely be calculated by using the help of Microsoft Office Excel. It is verified by; Chang Kyun-Oh (2007), which the true fracture strains, decreases sharply with increasing of the stress triaxiality. And by noting that the true fracture strain is found to be exponentially dependent on the stress triaxiality, thus the equation of true fracture strain ε_f can be calculated by first, calculating the stress triaxiality. The point when the pressure acted inside of the pipe is equal to burst pressure, is when value of equivalent strain is more than the value of true fracture strain; $\varepsilon_e > \varepsilon_f$.

Strees Triaxiality	Strain Min Princ	Strain Mid Princ	Strain Max Princ	1	2	3	surd(1+2+3)	equi. Strain	frac. Strain	burst pressure	Displacement	
0.844359	-0.06941314	-0.00146251	0.07375844	0.00461729	0.0204981	0.00565819	0.175424	0.08269567	0.9963491	31.49999955	1.3204845	
0.8328367	-0.086205088	-0.00173068	0.09088446	0.00713593	0.03136071	0.00857756	0.21696588	0.1022787	1.01239621	32.40000135	1.5156491	
0.8192326	-0.1092221	-0.0020683	0.1143063	0.01148194	0.04996495	0.01354305	0.27384289	0.12909078	1.03171282	33.30000045	1.7774915	
0.8044576	-0.14090925	-0.00252896	0.14652492	0.0191491	0.0826184	0.02221706	0.35211442	0.16598833	1.05315552	34.19999955	2.1270897	
0.7873064	-0.18575273	-0.0031659	0.19207025	0.03333795	0.1427502	0.03811716	0.46282319	0.21817695	1.0786665	35.09999865	2.5635359	
0.7629105	-0.25260106	-0.00402793	0.25983346	0.0617886	0.26258914	0.06962283	0.62769465	0.29589809	1.11613409	36.00000045	3.117065	
0.7354505	-0.34547019	-0.00499457	0.35372359	0.11592365	0.48887194	0.12867872	0.85643115	0.40372551	1.16002643	36.89999955	3.8841374	
0.7104377	-0.46695584	-0.00641311	0.47666627	0.21209961	0.89042269	0.23336569	1.1558062	0.54485227	1.2016549	37.79999865	5.0569086	
0.682967	-0.62209463	-0.00857125	0.63398045	0.37641094	1.57772461	0.41287269	1.53850844	0.72525984	1.24926017	38.70000045	6.5654254	
0.6505646	-0.82531977	-0.01146322	0.84008104	0.66236248	2.77355986	0.72512763	2.03986518	0.96160167	1.30806276	39.6	8.1643639	
0.6110351	-1.1269809	-0.01511364	1.1452851	1.2362488	5.16319277	1.34652524	2.78315771	1.31199312	1.38388878	40.4999991	10.056188	
0.48688	-1.5712343	-0.01940974	1.5931864	2.40815948	10.0135584	2.60046629	3.87584625	1.82709144	1.65440424	41.4000009	13.123577	Burst!!
0.3384036	-1.9046655	-0.02282369	1.9292562	3.54132861	14.6989556	3.81061588	4.69583859	2.21363954	2.05374115	42.3	17.479517	
0.3595669	-1.909987	-0.02291804	1.9347825	3.56102924	14.7822525	3.83259142	4.70912658	2.21990356	1.99109222	43.1999991	17.879974	
0.340722	-1.9057395	-0.02309695	1.9306155	3.54434296	14.7176197	3.81699235	4.69882485	2.21504728	2.046778	44.1000009	18.728453	
0.3575933	-1.8632149	-0.02325309	1.8883351	3.38545948	14.0741274	3.65416939	4.59497076	2.16608999	1.99684854	45	20.024529	

Figure 3.15: Determination of burst pressure

3.7 SCOPE OF OUTPUT

To make this project much meaningful in engineering criteria, a parametric study has been made to study the effect of pipe diameter and gouge depth to the value of burst pressure of the particular defective steel pipe. A variable of the diameter of pipe and the gouge depth are listed on the Table 3.2.

3.7.1 Parametric studies

For this project, a parametric study has been performed as in Table 3.2 to determine the burst pressure of the defective steel pipe and compare the effect when the pipe diameter and gouge depth were varied. Those diameters of pipe have been adapted specifically to the standards of the size of diameter from API. The gouge depth will be variable according to d/t=0.5.

Table 3.2: Variation of pipe diameter and gouge length for parametric study

Pipe No.	Pipe Length, *L* (mm)	Wall Thickness, *t* (mm)	Gouge Depth, *d* (mm)	*d/t*	Gouge Length, *l* (mm)
OD = 508 mm					
A	2300	17.5	8.75	0.5	100
B					200
C					300
D					400
OD = 762 mm					
E	2300	17.5	8.75	0.5	100
F					200
G					300
H					400
OD = 1016 mm					
I	2300	17.5	8.75	0.5	100
J					200
K					300
L					400

3.7.2 Gouge Defects

Figure 3.16 through 3.19 shows the different length of gouge defect on pipe model.

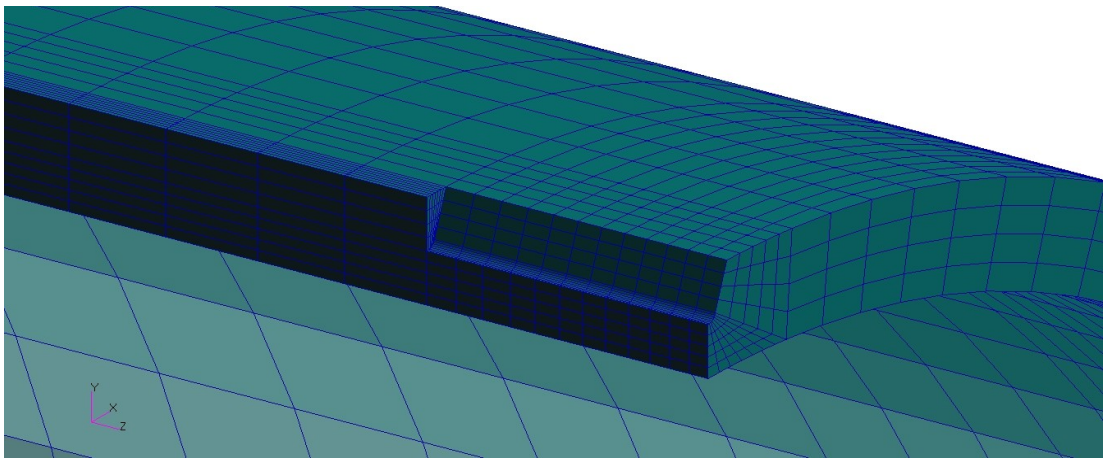

Figure 3.16: 100 mm gouge length on pipe model

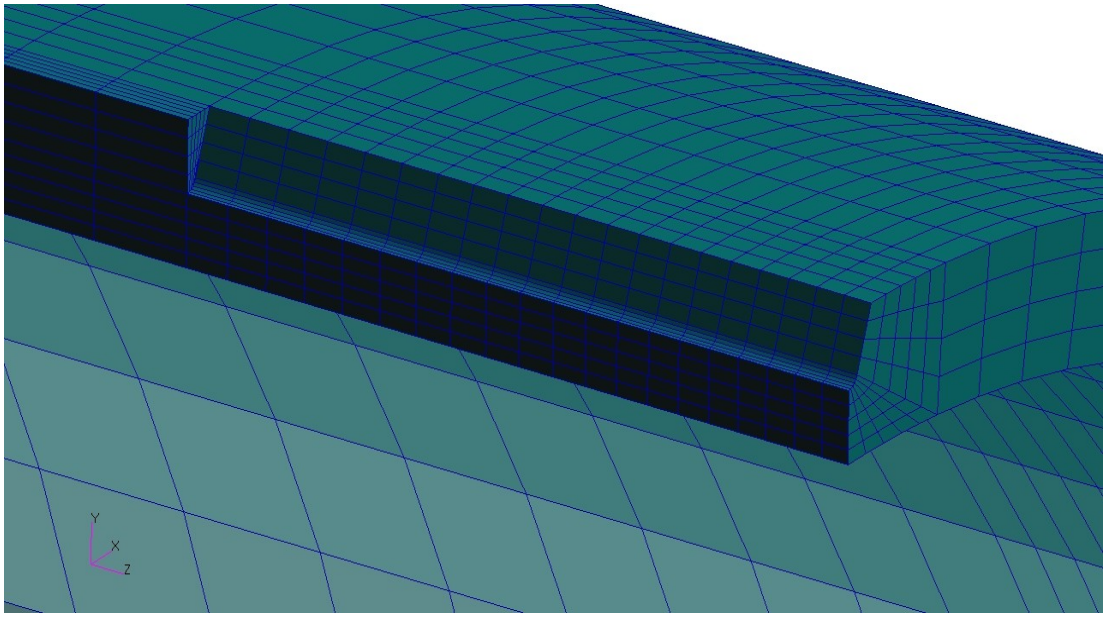

Figure 3.17: 200 mm gouge length

Figure 3.16 and 3.17 shows the gouge defect of length with 100 mm and 200 mm. While Figure 3.18 and 3.19 shows the defect length of 300 mm and 400 mm. Those four lengths of gouge defect was used in this thesis.

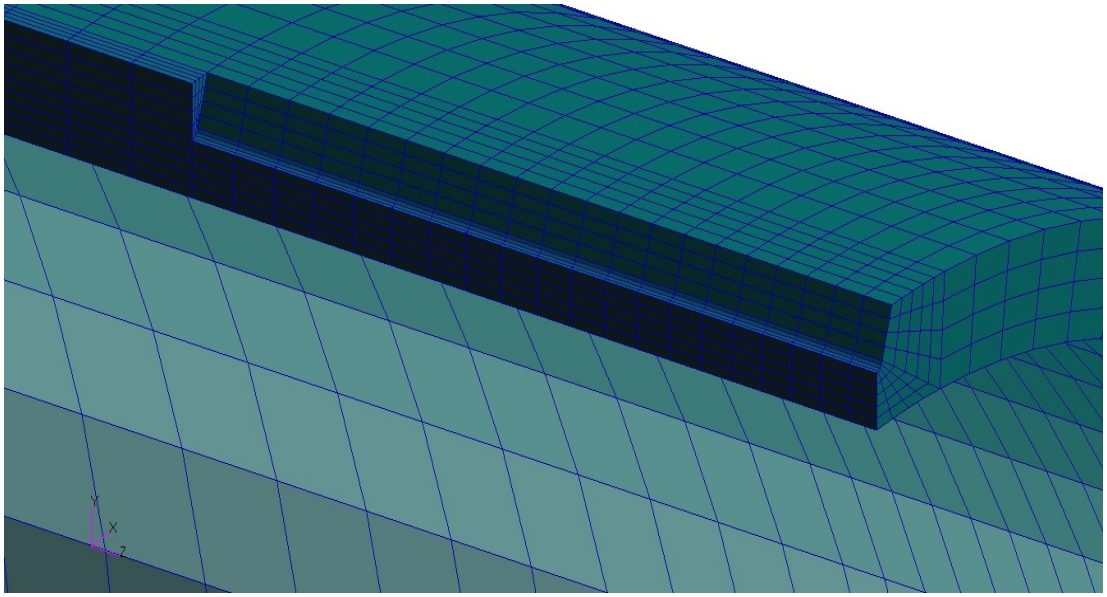

Figure 3.18: 300 mm gouge length

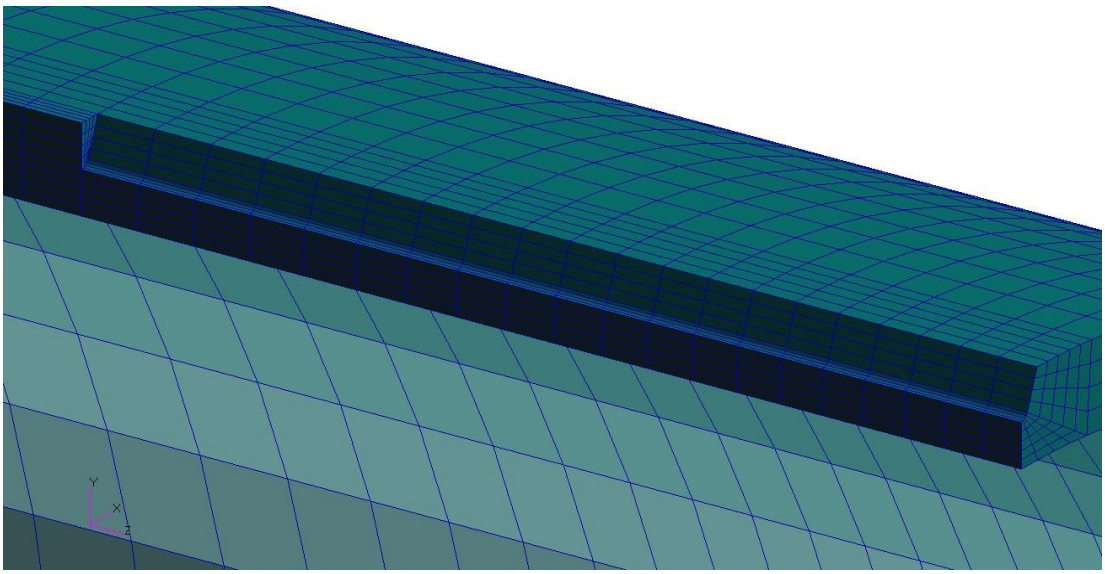

Figure 3.19: 400 mm gouge length

3.7.3 API RP FFS 579

Fitness for service assessment is performed to make sure that process plant equipment, such as pressure vessels, piping, and tanks, will operate safely and reliably for some desired future period. API Recommended Practice (RP) 579 provides a general procedure for assessing fitness for service. Local metal loss criteria were adapted to this research as a medium to predict the burst pressure of a gouged pipe. As in the API RP 579, Level 1 Assessment was used as the procedures to evaluate the pipe which subjected to internal pressure.

For level 1 assessment, burst pressure of a gouged pipe can be obtained using following equation,

$$P_f = P_b \left[\frac{R_t}{1 - \left(\frac{1}{M_t}\right)(1 - R_t)} \right] \tag{3.1}$$

P_b is the burst pressure of an intact pipe. For this value, each of every diameter of unflawed pipe was tested under internal pressure. R_t is the value of remaining thickness

ratio which given by equate from minimum thickness at gouge to the pipe wall thickness. As M_t is the Folias stress magnification factor,

$$M_t = \sqrt{\left(1+0.48\,\lambda^2\right)} \tag{3.2}$$

The shell parameter, λ, would be;

$$\lambda = \frac{1.285\,l}{\sqrt{ID \times t}} \tag{3.3}$$

Where,

l – Flaw length (gouge length); mm

ID – Internal Diameter of pipe; mm

CHAPTER 4

RESULTS AND DISCUSSION

4.1 Introduction

From the elastic-plastic deformation of the material, variation of stress triaxiality which leads to true fracture strains as a function of stress triaxiality can be obtained and used to determine the burst pressure of a notched steel pipe. By applying this burst pressure equation, the stresses subjected to the material due to the internal pressure of the pipe and the other stresses involved on outer surface of the pipe can be determine. But, in this project, the intention goes to the burst pressure of the API X65 steel pipe can withstand under the defective condition.

One-quarter symmetric conditions are fully utilized in this analysis to unsure the efficiency of computation of tested model. To avoid such problems with incompressibility, reduced integration element was applied to the properties of the model within MSC Patran. True stress-plastic strain data were used in the FE Analysis as shown in Figure 3.12. The material was modeled as an isotropic elastic-plastic material that obeys the incremental of plastic theory.

4.2 508 mm Outer Diameter Burst Result

Table 4.1: Result of burst pressure for pipe with OD = 508 mm

Pipe No.	Pipe Length, *L* (mm)	Wall Thickness, *t* (mm)	Gouge Depth, *d* (mm)	d/t	Gouge Length, *l* (mm)	Burst Pressure, P_b (MPa)	Displacement (mm)
A	2300	17.5	8.75	0.5	100	41.40	13.12
B					200	37.80	11.17
C					300	36.00	13.16
D					400	34.20	10.01

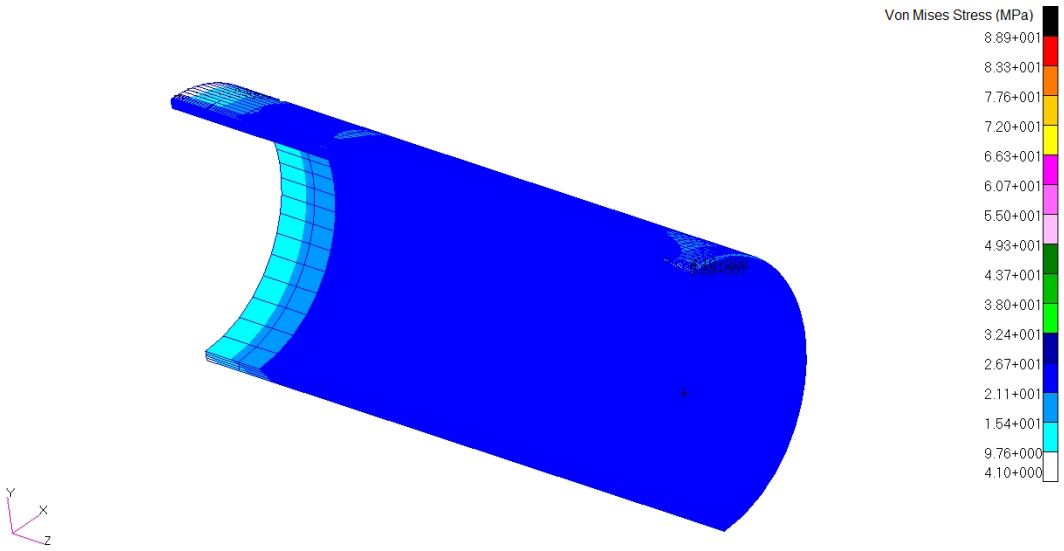

Figure 4.1: Von Mises stress distribution at internal pressure of 30 MPa

Table 4.1 shows the complete result of burst pressure and radial displacement at gouge tip for pipe with outer diameter of 508 mm. The result shows that, decrement of burst pressure is direct proportional to the increment of gouge length. As seen through Figure 4.2, the differences of burst pressure value from pipe B till pipe D are less significant.

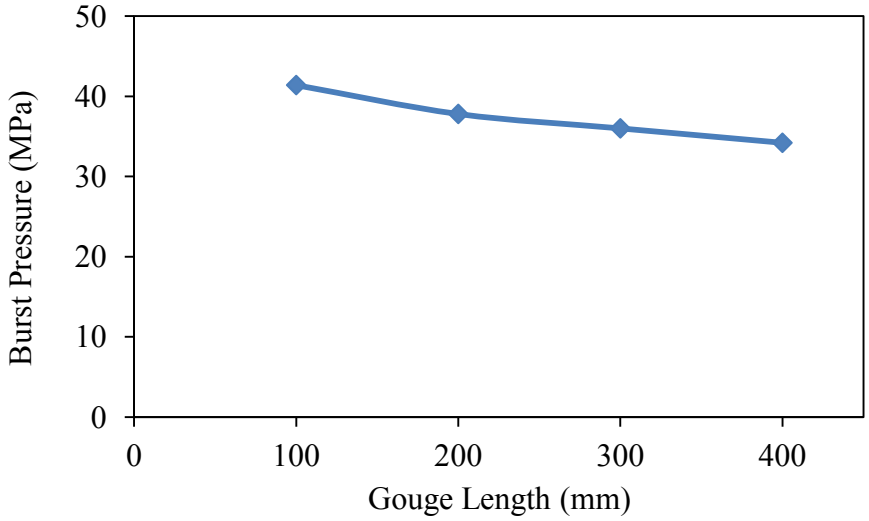

Figure 4.2: Effect of gouge length on burst pressure for pipe with OD = 508 mm

From the figure above, we can consider that the gouge length is stabilized at 200 mm. As it goes through 400 mm, the significance of difference is would be disregarded due to high burst pressure produced at 100 mm gouge length. For pipe case number of A and B gives 8.69 percent of pressure difference but for B and C and from C and D, the difference only takes at 4.76 percent and 5.00 percent. This can be said that as the difference is below than 5 percent of changes, the pipe can be assumed to be almost stabilized.

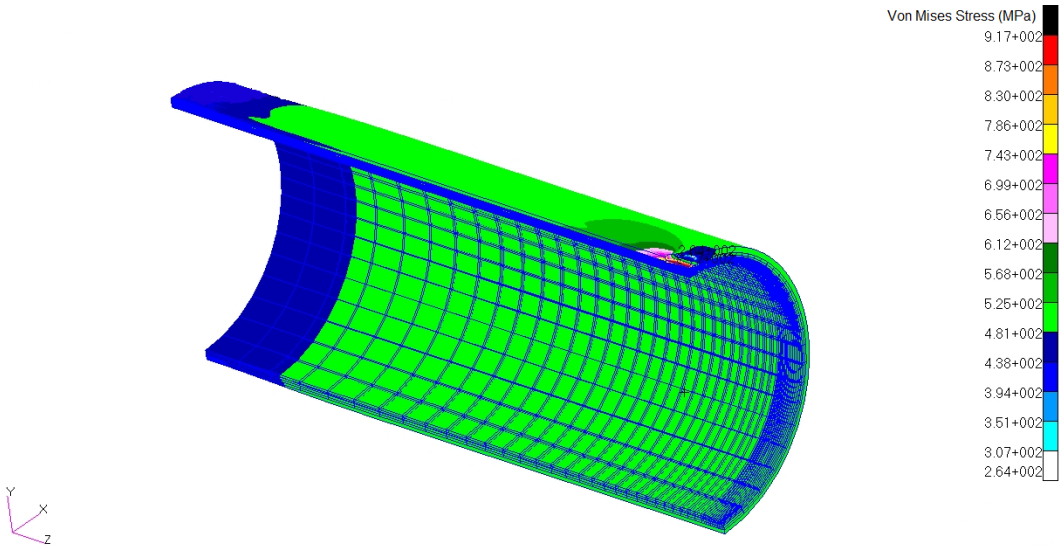

Figure 4.3: Final condition of pipe under internal hydrostatic pressure

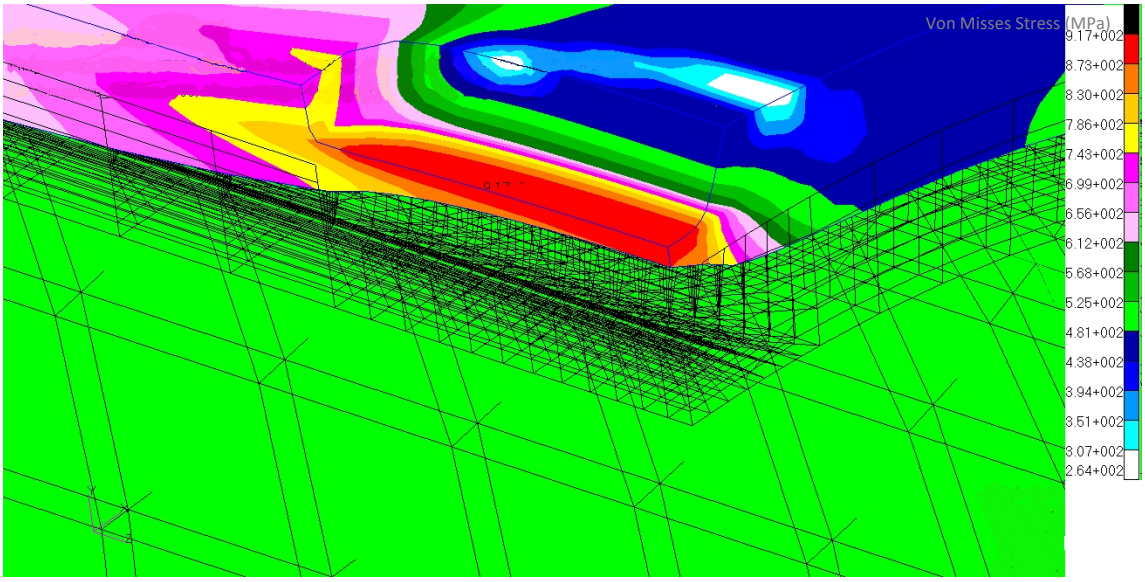

Figure 4.4: Close-up view of burst pipe

Figure 4.4 shows, as the defect is at burst state, the whole thickness of pipe is in red color. This indicates that the gouge is experiencing highest value of Von Misses Stress.

4.3 762 mm Outer Diameter Burst Result

Table 4.2: Result of burst pressure for pipe with OD = 762 mm

Pipe No.	Pipe Length, *L* (mm)	Wall Thickness, *t* (mm)	Gouge Depth, *d* (mm)	d/t	Gouge Length, *l* (mm)	Burst Pressure, P_b (MPa)	Displacement (mm)
D	2300	17.5	8.75	0.5	100	27.07	14.27
E					200	25.80	15.34
F					300	24.59	26.66
G					400	24.00	18.14

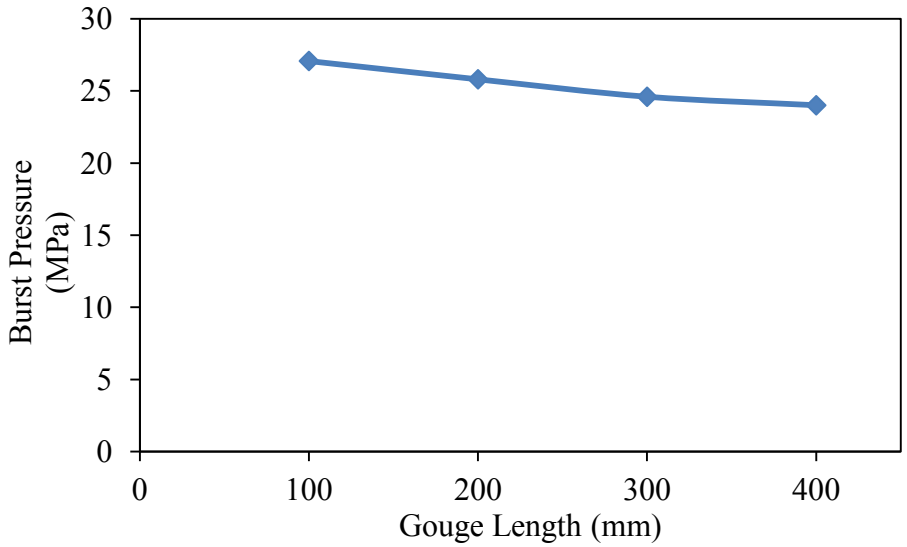

Figure 4.5: Effect of gouge length on burst pressure for pipe with OD = 762 mm

The maximum burst pressure experienced by the Outer Diameter of 762 mm is 27.07 MPa at 100 mm gouge length. As predicted, shortest gouge length will produce highest burst pressure. But for this case, as the gouge length increases from pipe case number of E through F, difference in burst pressure value does not varies significantly as it moves not more than 5 percent for every gouge length. Figure 4.5 shows the gradient of each every parameters does not contracts extremely as in outer diameter of 508 mm at pipe case number of A and B.

4.4 1016 mm Outer Diameter Burst Result

Table 4.3: Result of burst pressure for pipe with OD = 1016 mm

Pipe No.	Pipe Length, *L* (mm)	Wall Thickness, *t* (mm)	Gouge Depth, *d* (mm)	d/t	Gouge Length, *l* (mm)	Burst Pressure, P_b (MPa)	Displacement (mm)
I	2300	17.5	8.75	0.5	100	22.80	42.56
J					200	19.80	20.17
K					300	18.60	19.25
L					400	18.00	17.08

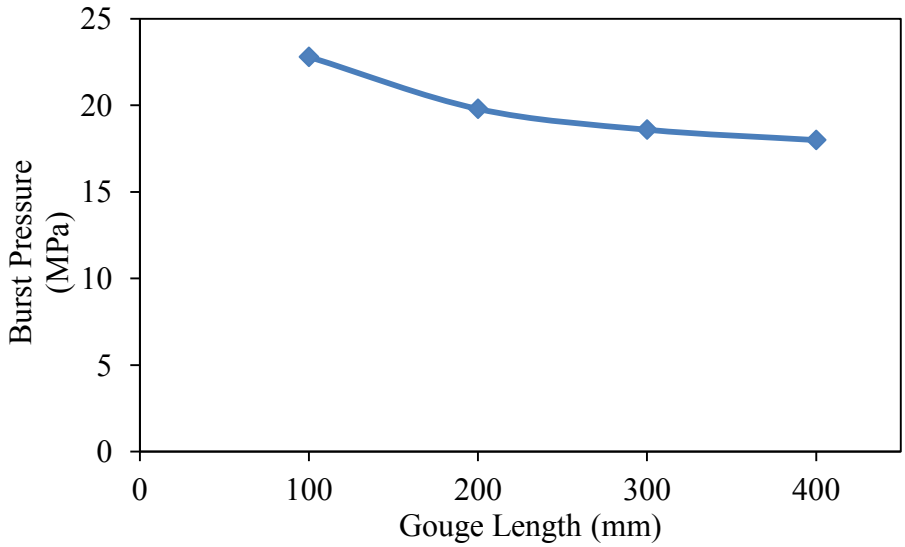

Figure 4.6: Effect of gouge length on burst pressure for pipe with OD = 1016 mm

Figure 4.6 particularly shows the declination trends of burst pressure as the increasing of gouge length from 100 mm through 400 mm for outer diameter of 1016 mm steel pipe. The difference is literally can be seen that as pipe case number I and J gives values of 13.16 percent of difference. This means, the burst pressure is still unstable for 100 mm length of gouge defect assessment. But, in the real-life, it can be considered as 100 mm length of gouge defect as safe because the pressure to reach burst state requires much more defect. As the length of defect goes from pipe J to K, the difference of burst pressure getting lower at 6.06 percent and 3.23 percent.

4.5 DISCUSSION

4.5.1 Summary of Burst Results

As the simulation ran, the results produced as in Figure 4.7 (a) and (b).

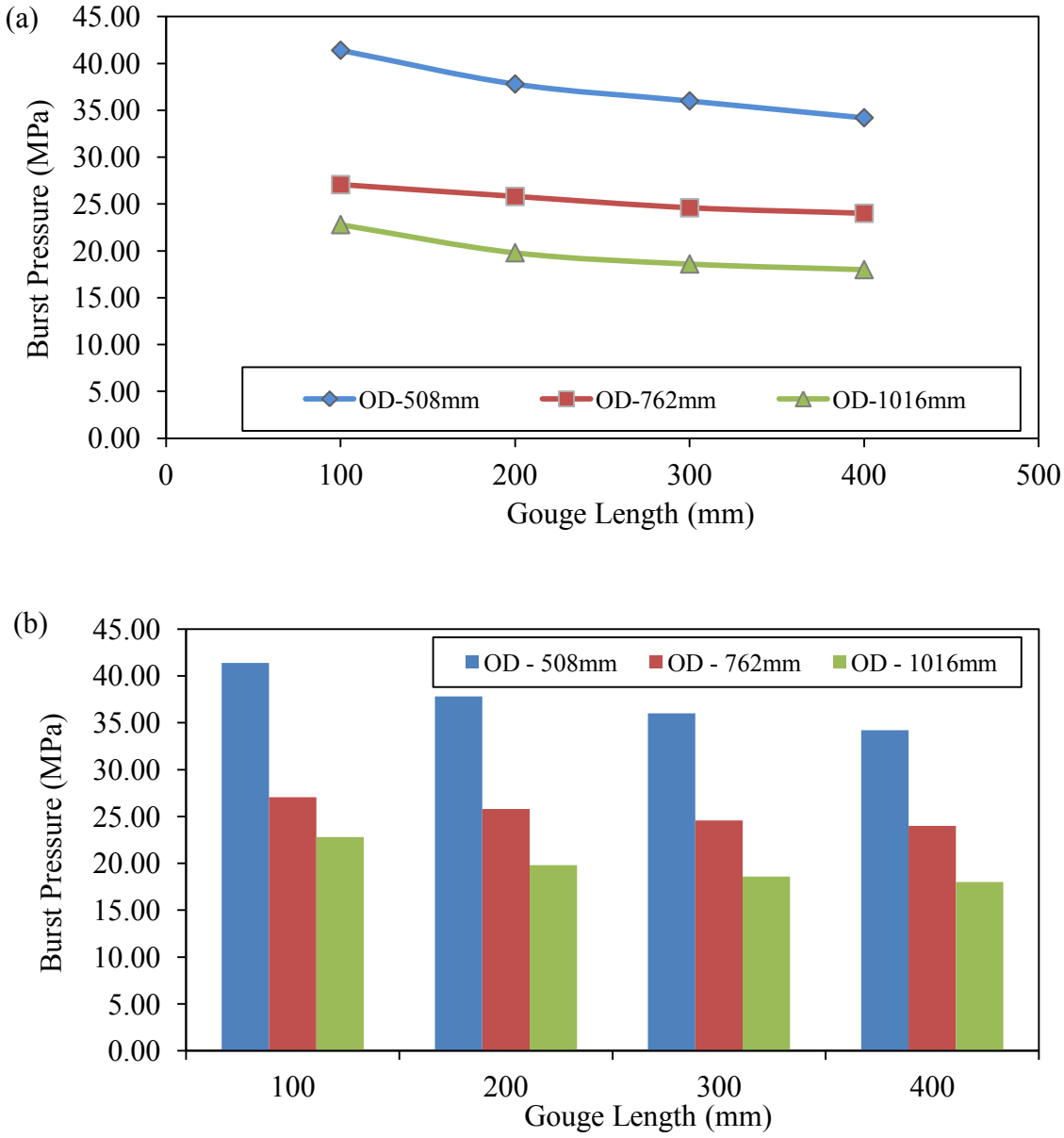

Figure 4.7: Summary of burst pressure

The pipe with smaller outer diameter gives higher burst pressure rather than other pipe with larger outer diameter (OD). This shows that the smaller pipe produces higher velocity of the product flows through it. It seems that, as the volume inside the pipe is directly proportional to the pressure acted to the internal wall of the pipe. Thus, low volume gives low pressure which in returns smaller OD in size produce larger burst pressure as it penetrates the gouge with reduced thickness.

As seen, the burst pressure resulted from OD of 762 mm and 1016 mm at 100mm gouge length does not different much. As the surface of cross sectional area in the pipe increases, the internal pressure would be decreases. It has been stated within the Pascal Law that pressure is indirect proportional to the surface area. But, to compare this two diameter pipe pressure difference is still identical although the diameter of pipe is not far too big in size. Looking to the Figure 4.8(a), the decrement trend of burst pressure for 762 mm and 1016 mm looks less sloppy rather than 508 mm.

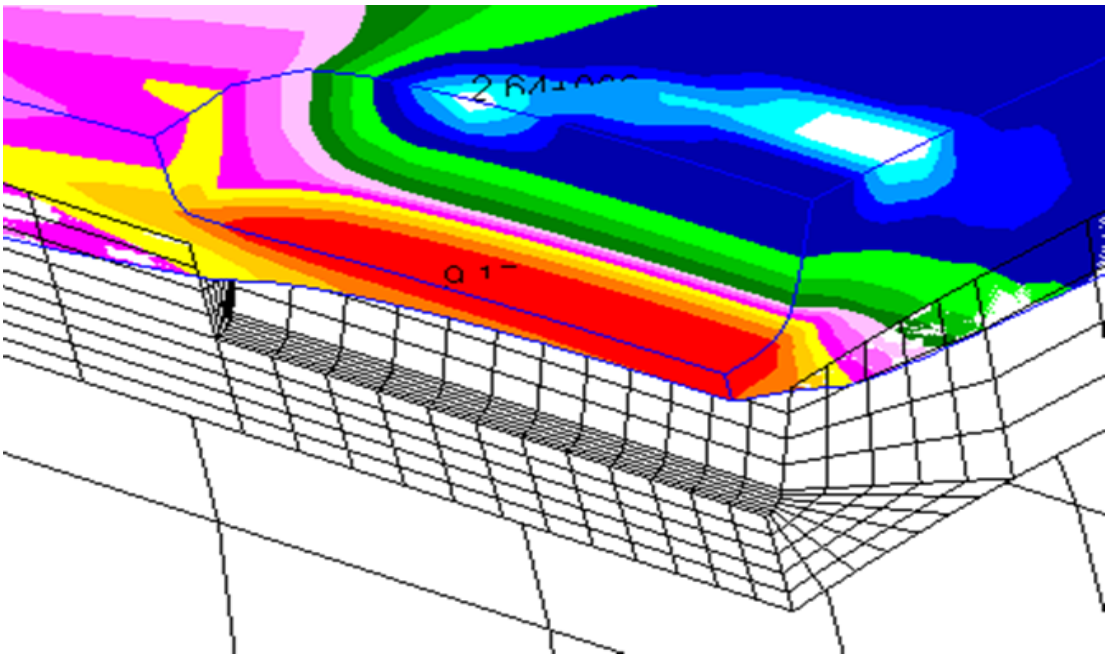

Figure 4.8: Defect on gouge tip

By comparing the gouge length through the same pipe OD as seen in Figure 4.8; taking OD of 1016 mm as an example. The burst pressure decreases as the gouge length increases. Means, as the length of reduced thickness section is increased, takes a slightly low pressure to burst the pipe at the critical point which takes place at the tip or the gouge defect. The critical point was assumed to be at the tip of the defect because higher stress loads can be assumed. Local wall thinning at the defect area makes the tip of defect, prone to fracture as the equivalent strain at the point exceeds the fracture strain.

4.5.2 Burst Pressure vs. Displacement

For the radial displacement of the defects, it was taken at the gouge tip. After burst happen under internal pressure, certain radial displacement can be obtained. Difference in radial displacement is dependent to the defect parameter. In certain situation, radial displacement also can be affected by the FE meshing details of the pipe with gouge.

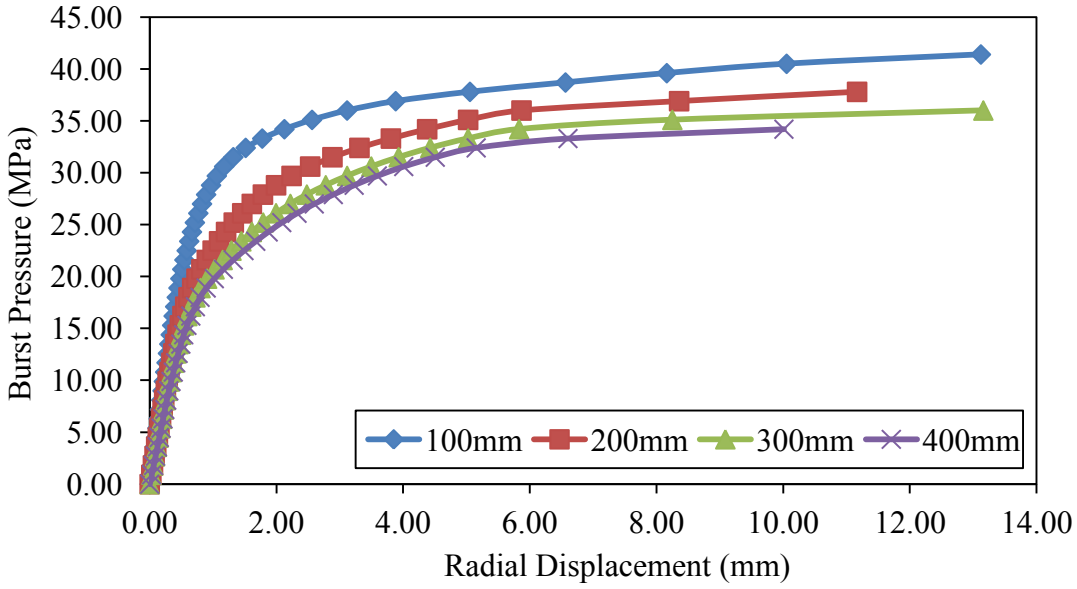

Figure 4.9: Effect of gouge length on radial displacement for pipe with OD = 508 mm

By referring to Figure 4.9, the trending shows displacement of critical point for variable gouge length does not directly increased as the gouge length increases. This was resulting from different meshing sizes for different cases of gouge length. As stated in Chapter 3, this analysis used critical location criterion which means, this analysis depends on the FE mesh sizes. Criterion based on the local critical location is a very mesh sensitive. It needs finer meshes to produce more conservative results and at which case, the value of burst pressure and radial displacement of gouge is much closer to the experiment or real-life situation. However, the usage of finer meshes requires much more of pipe modeling effort and also computational cost as it would make more matrices to the elements of the model.

Regarding of radial displacement for critical location, 300 mm gouge length gives highest value of radial displacement. For least value, 400 mm takes the place. As

the gouge length increases, the pressure needed to burst the pipe will also decrease. In return, lower pressure applied would make the pipe to burst early as compared to others which certainly makes the displacement of it is lower.

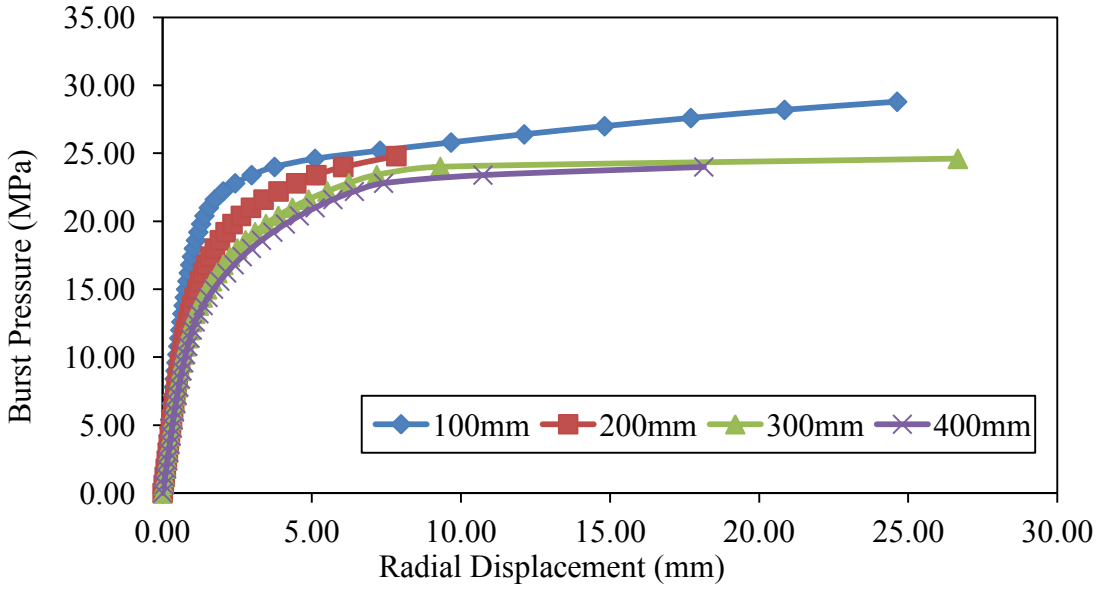

Figure 4.10: Effect of gouge length on radial displacement for pipe with OD = 762 mm

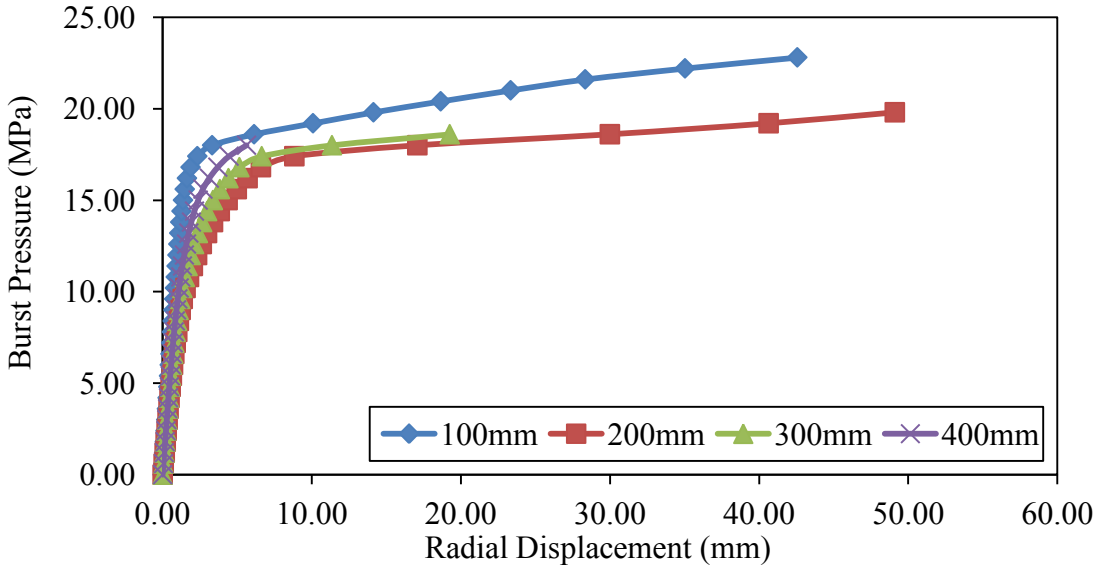

Figure 4.11: Effect of gouge length on radial displacement for pipe with OD = 1016 mm

It is well known that the defect would occur at ninety degree of the governing hoop stress to the cross-sectional plane due to the internal pressure. The ligament of fracture can be predicted to occur longitudinally through the pipe. As the internal pressure applied hydrostatically, the axial stress that holds the pipe at the initial geometry will expands. At the defect tip, principle stresses and strains increased as the pressure increased. The values through the hoop stress and radial stress were seen to fluctuate but the value of longitudinal stress is too small that can be neglected in the calculation. As the pressure increases, radial displacement at the defect tip also starts to increase.

4.6 Comparisons of Level 1 Assessment Code API 579 RP FFS

Level 1 assessment is a simple procedure to assess a component with a flaw which subjected to an internal pressure. This procedure can be used to determine the acceptability or to rerate a component with a flaw. As seen in the figure above, burst pressure of a flawed pipe produced by the API 579 code is slightly lower than the simulated burst pressure by the FEA. This could happen as the code considers the Folias stress magnification factor according to the shell parameter which includes the flaw dimension (gouge).

Table 4.4: 508 mm comparison with API RP FFS 579 code

OD (mm)	P_b (simulation, intact) (MPa)	l (mm)	λ	Rt	Mt	P_f (code-simulation, flawed) (MPa)	P_f (simulation, flawed) (MPa)
508	56.33	100.00	1.41	0.50	1.40	43.83	41.40
		200.00	2.82		2.20	36.46	37.80
		300.00	4.24		3.10	33.58	36.00
		400.00	5.65		4.04	32.14	34.20

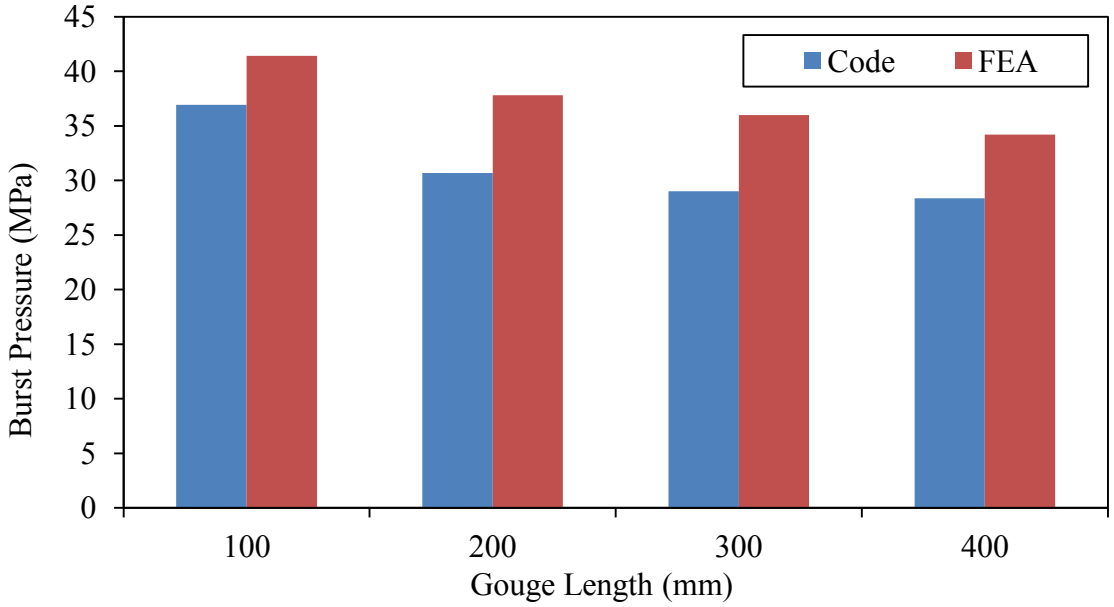

Figure 4.12: Comparison chart for OD 508 mm

Figure 4.12 shows the comparison chart for OD 508 mm, the total average percentage of difference of burst pressure value between code and simulation is 16.53 percent. From each of the gouge length parameters, the increment of difference percentage shows that it is not increased on a straight line. This could happen when the gouge length at 300 mm could be established as a stabilized gouge defect and if the length was increased more than 400 mm, the pressure for the pipe to burst will not move much.

Table 4.5: 762 mm comparison with API RP FFS 579 code

OD (mm)	P_b (simulation, intact) (MPa)	l (mm)	λ	Rt	Mt	P_f (code-simulation, flawed) (MPa)	P_f (simulation, flawed) (MPa)
762	33.25	100.00	1.14	0.50	1.27	27.37	27.07
		200.00	2.28		1.87	22.70	25.80
		300.00	3.42		2.57	20.64	24.59
		400.00	4.56		3.31	19.58	24.00

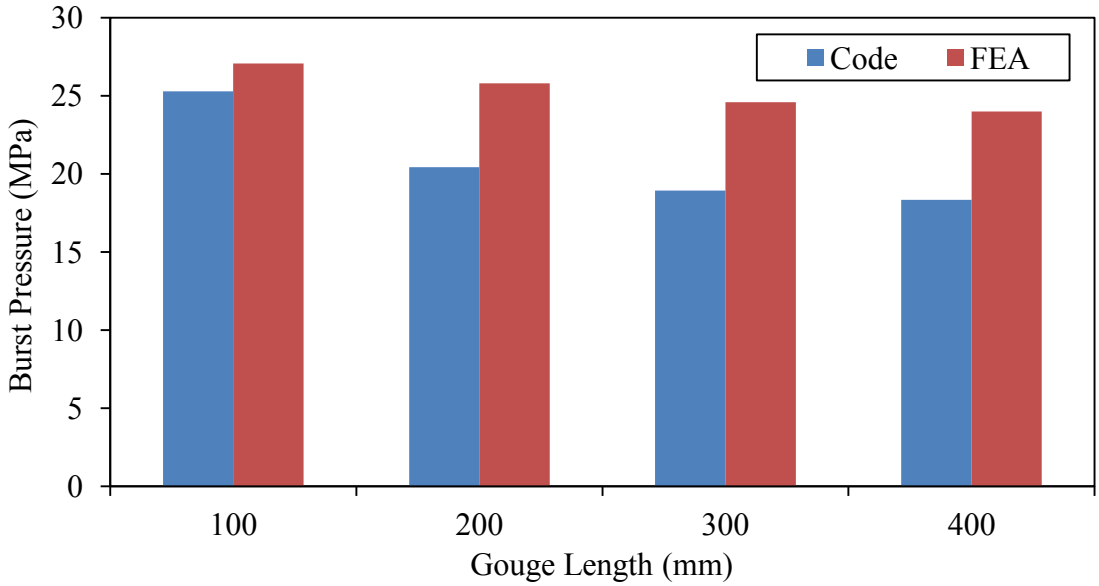

Figure 4.13: Comparison chart for 762 mm

Figure 4.13 shows the comparison between code and FEA for OD of 762 mm, the total average percentage of difference of burst pressure value between code and simulation is 18.5 percent. From each of the gouge length parameters, the increment of difference percentage shows that it is not increased on a straight line. This maybe will take place when the gouge length at 300 mm could be recognized as a stabilize gouge defect and if the length was greater than before, the pressure difference would not be identical.

Table 4.6: 1016 mm comparison with API RP FFS 579 code

OD (mm)	P_b (simulation, intact) (MPa)	l (mm)	λ	Rt	Mt	P_f (code-simulation, flawed) (MPa)	P_f (simulation, flawed) (MPa)
1016	26.58	100.00	0.98	0.50	1.21	22.66	22.80
		200.00	1.96		1.69	18.89	19.80
		300.00	2.94		2.27	17.04	18.45
		400.00	3.92		2.90	16.06	18.00

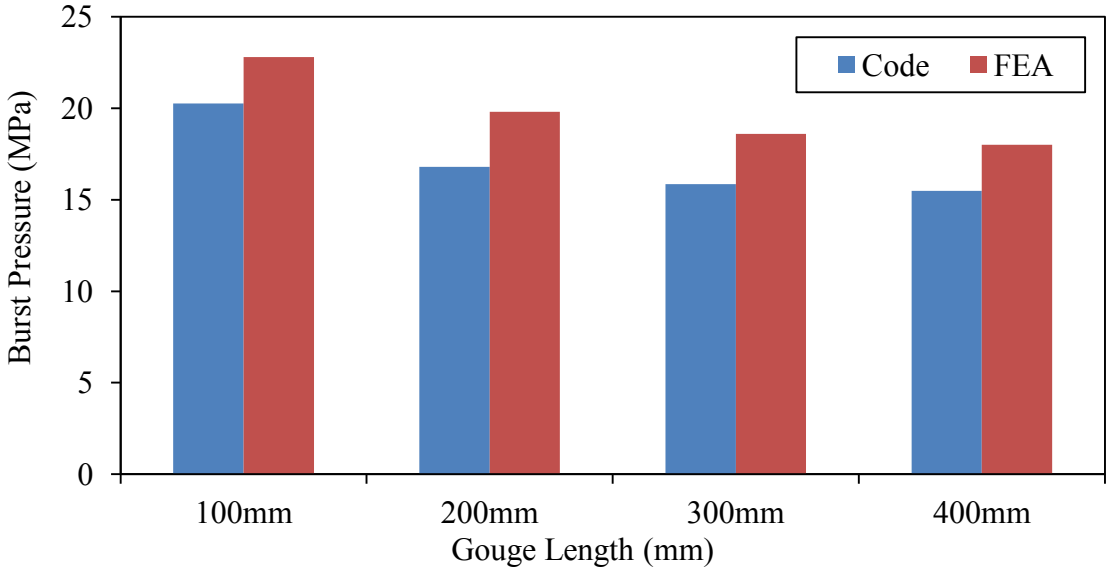

Figure 4.13: Comparison chart for 1016 mm

From Figure 4.13, the comparison for OD of 1016 mm shows the total average percentage of difference of burst pressure value between code and simulation is 13.58 percent. From each of the gouge length parameters, the increment of difference percentage shows that it is not increased on a straight line. This could happen when the gouge length at 300 mm could be establish as a stabilize defect and if the length was extended more than 400 mm, the pressure for the pipe to fracture will not move to a great extent.

CHAPTER 5

CONCLUSION AND RECOMMENDATION

5.1 CONCLUSION

In this thesis, the value of burst pressure has been analyzed for a gouge defect API X 65 steel pipes. FE analysis data has been collected from the solver, MSC Marc, through the post-processer, MSC Patran and the result of burst pressure was calculated using Microsoft Excel 2011.

For the result obtained, OD parameter of 508 mm gives the highest value of burst pressure rather than 762 mm and 1016 mm. These shows that burst pressure values decrease as the diameter of pipe increases. It was proven that 508 mm of OD gives highest burst pressure at 41.40 MPa with a 100 mm length of gouge. As 1016 mm OD gives lowest value of burst pressure at 22.80 MPa at same length of gouge which produce difference 18.60 MPa.

As gouge length was also made as the study parameter, difference of burst pressure through 4 different lengths was identified with each 508 mm, 762 mm and 1016 mm. Burst pressure shows the highest value when the defect is at 100 mm length. As the length increases to 200 mm the burst pressure drops significantly. Burst pressure for gouge length of 300 mm and 400 mm does not differ much which only produce about 5 percent of differences.

5.2 RECOMMENDATION

For future work, will concentrate on other defect type such as corrosion or dents with different parameters with the usage of much more finer mesh size to obtain more conservative model to be analyzed. It is also suggested to include experimental test data to be compared with FE analysis results.

Besides that, in this study, a few factors such as pipe material or type of pipe have been specifically chosen. So, for further study criteria it is strongly recommended to analyze the type of pipe used in oil and gas transportation with focused within Malaysia. Other than that, if corrosion defect has been taken as a defect type, metallographic study is recommended to be done for each corresponding pipe used in the study.

REFERENCES

American Petroleum Institute. 2000. *Specification for line pipe.*

API 579. 2000. *Recommended Practice for Fitness of Service*. First Edition.

Beer FP, Jr. Johnston ER, DeWolf JT. 2006. *Mechanics of Material*. Fourth edition in SI unit. Kuala Lumpur: McGraw-Hill Higher Education.

Budynas RG, Nisbett JK. 2008. *Shigley's mechanical engineering design*. Eight Edition in SI Unit. Singapore: McGraw-Hill Higher Education.

Clausing DP. 1970. Effect of plastic strain state on ductility and toughness. *International Journal of Fracture Mechanics.* **6**:71-85.

Cosham A, Hopkins P. 2004. The effect of dents in pipeline – guidance in the pipeline defect assessment manual. *International Journal of Pressure Vessels and Piping.* **81**: 127-139.

Kamaya M, Suzuki T, Meshii T. 2008. Failure pressure of straight pipe with wall thinning under internal pressure. *International Journal of Pressure Vessels and Piping.* **85**: 628-634.

Mackenzie AC, Hancock JW, Brown DK. 1977. On the influence of state of stress on ductile failure initiation in high strength steels. *Engineering Fracture Mechanics.* **9**: 167-188.

McClintock FA. 1968. A criterion of ductile fracture by the growth of holes. *Journal of Applied Mechanics.* **35**: 363-371.

Oh CK, Kim YJ, Baek JH, Kim WS. 2007. Development of stress-modified fracture strain for ductile failure of API X65 steel. *International Journal of Fracture*. **143:** 119-113.

Oh CK, Kim YJ, Baek JH, Kim WS, Kim YP. 2007. Ductile failure analysis of API X65 pipes with notch-type defects using a local fracture criterion. *International Journal of Pressure Vessels and Piping.* **84**: 512-525.

Rice JR, Tracey DM. 1969. On ductile enlargement of voids in triaxiality stress fields. Journal of Physics and Mechanic Solids. **17**:201-217.

Roylance D. 2001. *Stree-Strain curve*. Department of Material Science and Engineering.

APPENDIX A

GANTT CHART

A1

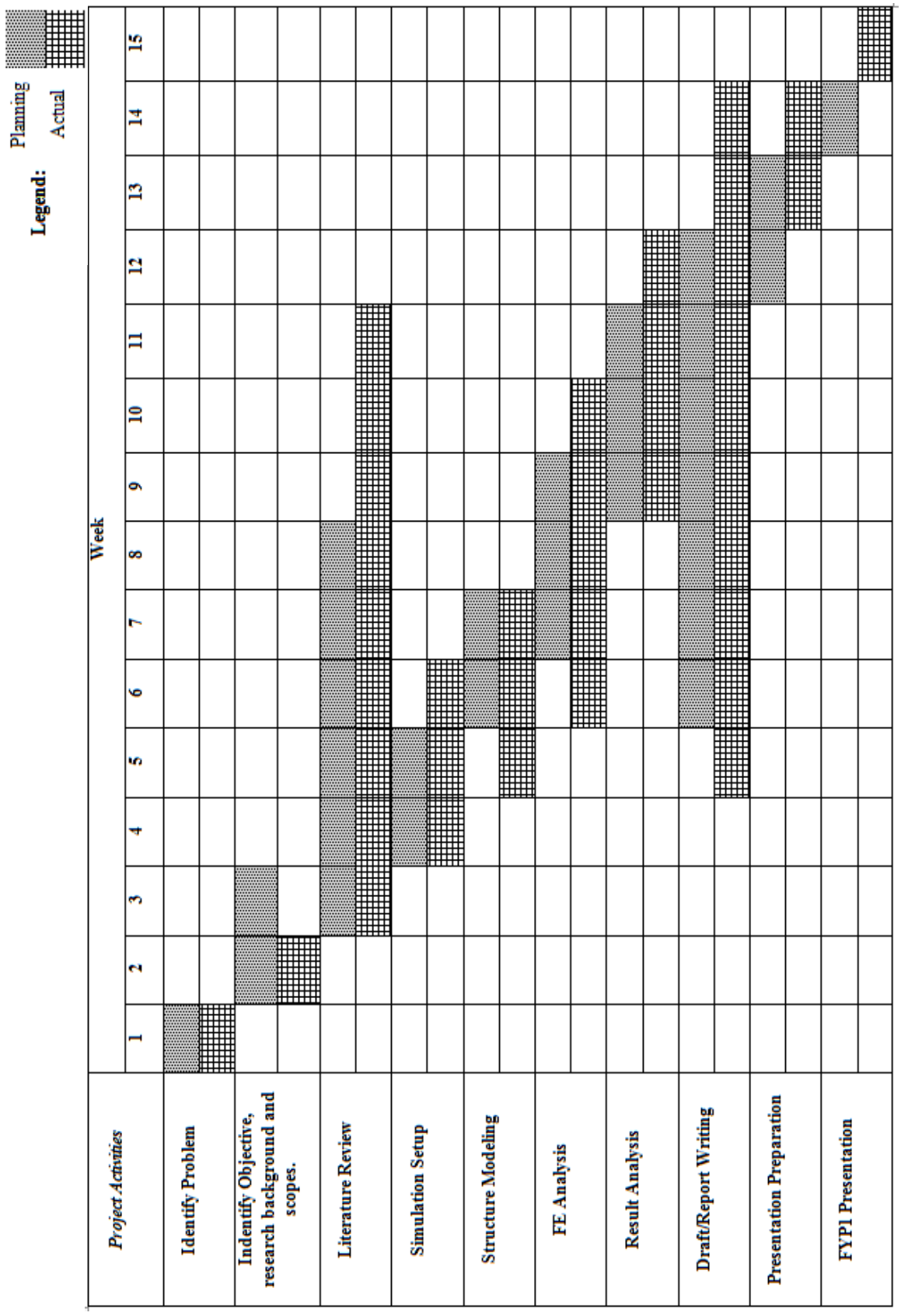

A2

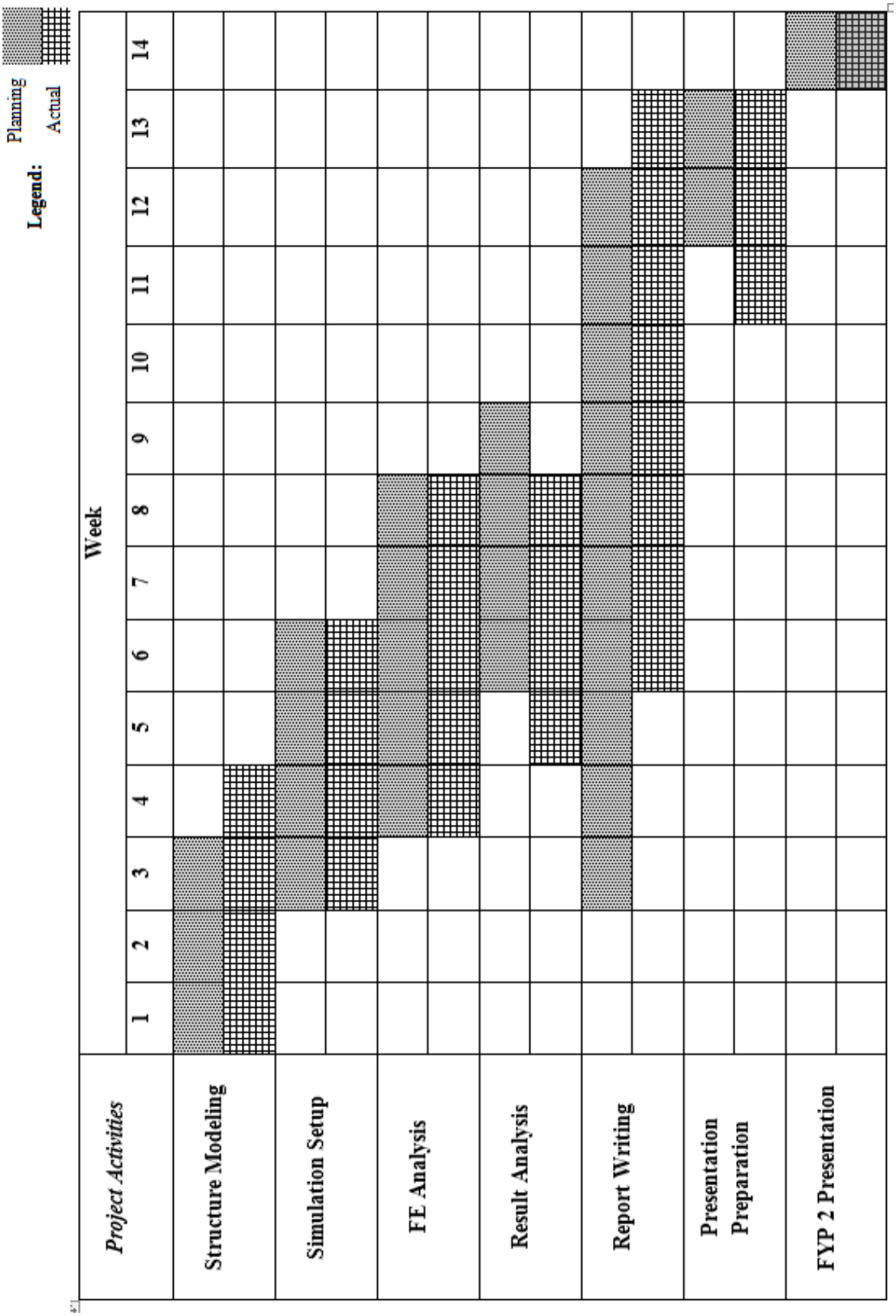
Legend:
Planning
Actual
Week
Project Activities
1
2
3
4
5
6
7
8
9
10
11
12
13
14
Structure Modeling
Simulation Setup
FE Analysis
Result Analysis
Report Writing
Presentation Preparation
FYP 2 Presentation